European Journal of Medicinal Chemistry 215 (2021) 113252

Contents lists available at ScienceDirect

European Journal of Medicinal Chemistry

journal homepage: http://www.elsevier.com/locate/ejmech

Design of pyrido[2,3-d]pyrimidin-7-one inhibitors of receptor interacting protein kinase-2 (RIPK2) and nucleotide-binding oligomerization domain (NOD) cell signaling

Sameer Nikhar [a], Ioannis Siokas [b], Lisa Schlicher [c], Seungheon Lee [a], Mads Gyrd-Hansen [c], Alexei Degterev [b, *], Gregory D. Cuny [a, **]

[a] Department of Pharmacological and Pharmaceutical Sciences, University of Houston, Health Building 2, Houston, TX, 77204, USA
[b] Department of Developmental, Molecular & Chemical Biology, Tufts University School of Medicine, 136 Harrison Avenue, Boston, MA, 02111, USA
[c] Nuffield Department of Medicine, Ludwig Institute for Cancer Research, University of Oxford, Old Road Campus, Roosevelt Drive, OX3 7DQ, UK

ARTICLE INFO

Article history:
Received 11 December 2020
Received in revised form
28 January 2021
Accepted 29 January 2021
Available online 3 February 2021

Keywords:
Inhibitor
Kinase
NOD
Nucleotide-binding oligomerization domain
Pyrido[2,3-d]pyrimidin-7-one
Receptor-interacting protein kinase 2
RIPK2

ABSTRACT

Receptor interacting protein kinase-2 (RIPK2) is an enzyme involved in the transduction of pro-inflammatory nucleotide-binding oligomerization domain (NOD) cell signaling, a pathway implicated in numerous chronic inflammatory conditions. Herein, a pyrido[2,3-d]pyrimidin-7-one based class of RIPK2 kinase and NOD2 cell signaling inhibitors is described. For example, **33** (e.g. **UH15**–**15**) inhibited RIPK2 kinase (IC_{50} = 8 ± 4 nM) and displayed > 300-fold selectivity versus structurally related activin receptor-like kinase 2 (ALK2). This molecule blocked NOD2-dependent HEKBlue NF-κB activation (IC_{50} = 20 ± 5 nM) and CXCL8 production (at concentrations > 10 nM). Molecular docking suggests that engagement of Ser25 in the glycine-rich loop may provide increased selectivity versus ALK2 and optimal occupancy of the region between the gatekeeper and the αC-helix may contribute to potent NOD2 cell signaling inhibition. Finally, this compound also demonstrated favorable *in vitro* ADME and pharmacokinetic properties (e.g. C_{max} = 5.7 μM, T_{max} = 15 min, $t_{1/2}$ = 3.4 h and Cl = 45 mL/min/kg following single 10 mg/kg intraperitoneal administration) further supporting the use of pyrido[2,3-d]pyrimidin-7-ones as a new structure class of RIPK2 kinase and NOD cell signaling inhibitors.

1. Introduction

Receptor interacting protein kinase-2 (RIPK2), also known as RICK/CARDIAK/CARD3, is a dual serine/threonine and tyrosine kinase that plays a pivotal role in signal transduction from nucleotide-binding oligomerization containing proteins 1/2 (NOD1/2) [1,2]. These two proteins are cytosolic receptors and part of the pattern recognition receptor family along with Toll-like receptors that cause activation of nuclear factor κ-light chain enhancer of activated B cells (NF-κB) in immune cells after bacterial invasion. These cytosolic proteins detect bacterial peptidoglycan fragments, namely diaminopimelic acid (DAP) and muramyl dipeptide (MDP), present in Gram-positive and Gram-negative bacteria [3]. Upon activation, NOD1/2 binds to RIPK2 through its caspase activation and recruitment domain (CARD) propagating pro-inflammatory signaling [4]. RIPK2 undergoes autophosphorylation of its kinase domain and binds to X-linked inhibitor of apoptosis proteins (XIAP) and other E3 ubiquitin ligases for non-degradative polyubiquitination [5]. Polyubiquitinated RIPK2 then activates transforming growth factor beta-activated kinase 1 (TAK1) and IκB kinase complex (IKK) causing upregulation of mitogen-activated protein kinases (MAPK) and NF-κB. Activation of NF-κB results in transcription of multiple pro-inflammatory cytokine genes [6].

Normal regulation of the NOD1/2-RIPK2 signaling cascade is beneficial in providing defense against invading bacteria. But dysregulation, including a genetic mutations in NOD1/2, may cause excessive RIPK2 activation and thereby contribute to inflammation in multiple conditions, such as inflammatory rheumatoid arthritis and Blau syndrome and in neuro-inflammatory conditions (e.g. multiple sclerosis) [7,8]. Small molecule pharmacological probes for RIPK2/NOD signaling would be useful for furthering the

* Corresponding author.
** Corresponding author.
E-mail addresses: alexei.degterev@tufts.edu (A. Degterev), gdcuny@central.uh.edu (G.D. Cuny).

https://doi.org/10.1016/j.ejmech.2021.113252
0223-5234/

understanding of this pathway and may provide a foundation for therapeutic development.

Several RIPK2 kinase inhibitors have been reported in the literature, including SB203580 (**1**) [9], Gefitinib (**2**) [10], OD36 (**3**) and OD38 (**4**) [11], WEHI-345 (**5**) [12], Ponatinib (**6**) [13], GSK583 (**7**) [14], **8a** and its pro-drug **8b** [15], **9** and **10** [16], and **11** [17] (Fig. 1). Recently, our laboratory identified another class of potent RIPK2/NOD signaling inhibitors based on a 3,5-diaryl-2-aminopyridine scaffold, exemplified by CSLP37 (**12**) [18]. This latter class of compounds was shown to disrupt XIAP-RIPK2 interactions mitigating NOD2 inflammatory signaling [19]. Furthermore, these studies demonstrated that impairing RIPK2 ubiquitination was critical for functional activity, as opposed to blocking catalysis per se. Herein, we describe a structurally distinct class of pyrido[2,3-d]pyrimidin-7-one RIPK2 inhibitors. Importantly, optimization of the solvent exposed region and appropriate occupancy of the region between the gatekeeper and the αC-helix were necessary to achieve potent NOD2 cell signaling inhibition as assessed in NF-κB activation HEKBlue and pro-inflammatory CXCL8 production assays. These compounds will contribute to the collective molecular toolset of RIPK2/NOD signaling inhibitors for further elucidation of this emerging therapeutic paradigm.

2. Compound design and synthesis

During an activin receptor-like kinase 2 (ALK2) screening campaign, the pyrido[2,3-d]pyrimidin-7-one PD180970 (**13**) was identified as a modest inhibitor (ALK2 IC_{50} ~ 1 μM). This compound has previously been reported to bind Abl kinase in a conformational state intermediate between DFG-in and DFG-out [20]. Addition of a solubilizing group as in PD166285 (**14**) [21] provided potent ALK2 inhibition (IC_{50} = 0.021 ± 0.016 μM) (Fig. 2A). We and others have found that various ALK2 inhibitors oftentimes demonstrate inhibitory activity against RIPK2 [22,23]. In the case of **14**, RIPK2 was indeed potently inhibited (IC_{50} = 0.013 ± 0.004 μM). In addition, the compound blocked NOD2 cell signaling (IC_{50} = 0.037 ± 0.004 μM) in the HEKBlue assay of NOD2-dependent NF-κB activation in response to L18-MDP stimulation. Encouraged by these results, a structure-activity relationship (SAR) analysis was conducted examining several regions of the pyrido [2,3-d]pyrimidin-7-one scaffold (Fig. 2B) assessing RIPK2 and ALK2 kinase inhibitory activities, as well inhibition of NOD2 cell signaling via the HEKBlue assay. One specific direction of the SAR study was to introduce a sulfone as a hydrogen bond acceptor to engage Ser25 in the glycine-rich loop of RIPK2 that is only present in three other kinases [24], as was previously done with **7**–**10** [14–16].

Compounds used for the SAR analysis were synthesized using 2-(methylthio)-6-phenylpyrido[2,3-d]pyrimidin-7-one intermediates that were generated via two different routes. For the first method, the synthesis of the 6-(2,4-dichlorophenyl)-8-methyl-2-(methylthio)pyrido[2,3-d]pyrimidin-7(8H)-one (**A9a**) started with the commercially available ethyl-4-chloro-2-(methylthio)pyrimidine-5-carboxylate (**A1**) as shown in Scheme 1. This material was either treated with ammonium hydroxide in the presence of triethylamine (TEA) to furnish **A2** in 98% yield or with aqueous methylamine to generate **A3** in 85% yield. The ethyl esters were reduced in the presence of lithium aluminum hydride (LAH) to provide the corresponding alcohols **A4** and **A5** in 61% and 95% yield, respectively. The alcohols were then treated with manganese dioxide to obtain the aldehydes **A6** and **A7** in 83% and 95% yield, respectively. Oxidation of alcohol **A5** to **A7** was also performed using Dess-Martin periodinane, but the yield was lower (i.e. 56%). Condensation of **A7** with different phenylacetonitriles in the presence of potassium carbonate generated pyrido[2,3-d]pyrimidine-7-

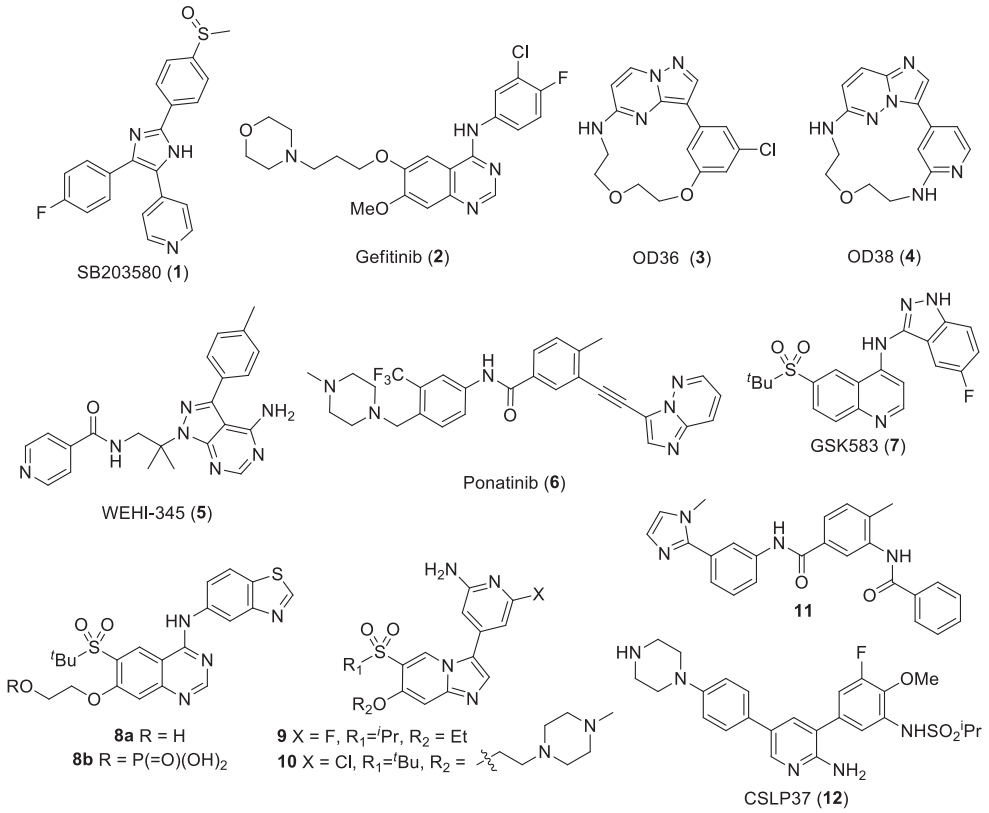

Fig. 1. Previously reported RIPK2 kinase inhibitors.

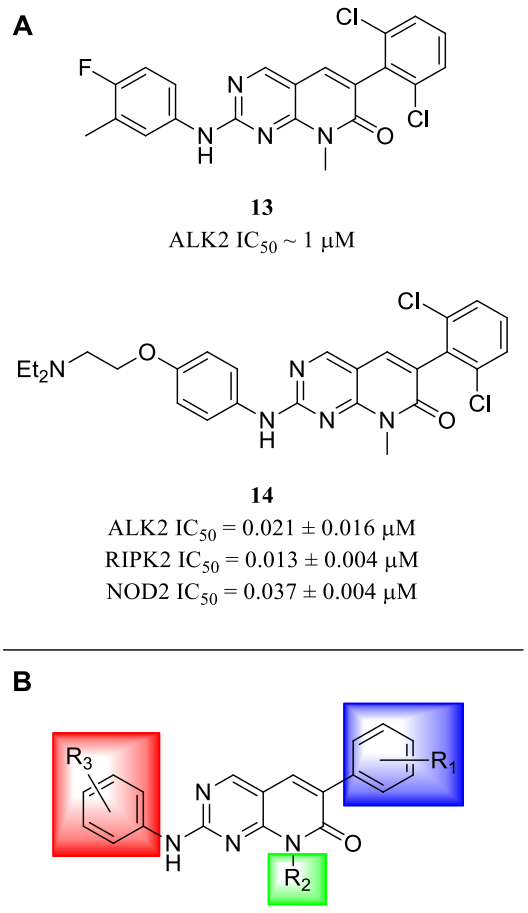

Fig. 2. (**A**) Structures of **13** and **14**, as well as a summary of ALK2, RIPK2 kinase and NOD cell signaling inhibitory data. (**B**) Regions of the pyrido[2,3-d]pyrimidin-7-one scaffold explored for SAR analysis.

imines **A8a-c** in 54–63% yield. The imines were then converted to the corresponding pyrido[2,3-d]pyrimidin-7-ones **A9a-c** in 55–65% yields through sequential *N*-acetylation with acetic anhydride followed by hydrolysis with concentrated hydrochloric acid (HCl) [25,26]. Although this method produced several of the desired pyrido[2,3-d]pyrimidine-7-ones, it was not particularly efficient.

Alternatively, pyrido[2,3-d]pyrimidine-7-ones were synthesized by condensing **A6** or **A7** with substituted phenylacetate esters in the presence of KF/Al_2O_3 to furnish **A9d-j** in 30–60% yield, as shown in Scheme 2 [27]. Furthermore, intermediate **A10** was deprotonated with sodium hydride (NaH) and then exposed to different alkyl iodides to furnish **A9m-t** in 28–74% yield. The 4-hydroxyphenyl derivative **A9j** was treated with t-butyldimethylsilyl chloride in the presence of dimethylaminopyridine (DMAP) and imidazole or methylated with methyl iodide in the presence of potassium carbonate to afford **A9k** and **A9l** in 88% and 95% yield, respectively.

The various 2-(methylthio)-6-phenylpyrido[2,3-d]pyrimidin-7-ones **A9a-i** and **A9k-t** were oxidized using *m*-chloroperbenzoic acid (*m*-CPBA) to afford methyl sulfones **A11a-i** and **A11k-t** in 40–93% yield (Scheme 3). Initial attempts to displace the methyl sulfones with anilines did not furnish the desired products. Alternatively, the anilines **A12a-c** were converted to their corresponding formamides **A13a-c** by heating in formic acid, then deprotonated with sodium hydride followed by treatment with methyl sulfones to generate the desired compounds in 33–95% yield [28].

In a case where requisite phenylacetate esters were not readily available, an alternative synthetic method was pursued as illustrated in Scheme 4. Intermediate **A7** was treated with ethyl 2-chloro-2-(diethoxyphosphoryl)acetate to give **A14** in 42% yield [29]. This was followed by coupling **A14** with the commercially available 2-chloro-4-methylphenylboronic acid under Suzuki conditions to afford **A15** in a 57% yield. Furthermore, oxidation of **A15** with *m*-CPBA gave **A16** in 68% yield, which upon treatment with the anion of **A13c** generated in the presence of NaH gave **38** in 75% yield.

3. Results and discussion

To increase the selectivity for RIPK2 versus ALK2 while maintaining cellular potency, the hydrophobic substitutions (R_1) at different positions on the phenyl ring, which projects towards the glutamate residue of the α-C helix in the docking model (Fig. 4A),

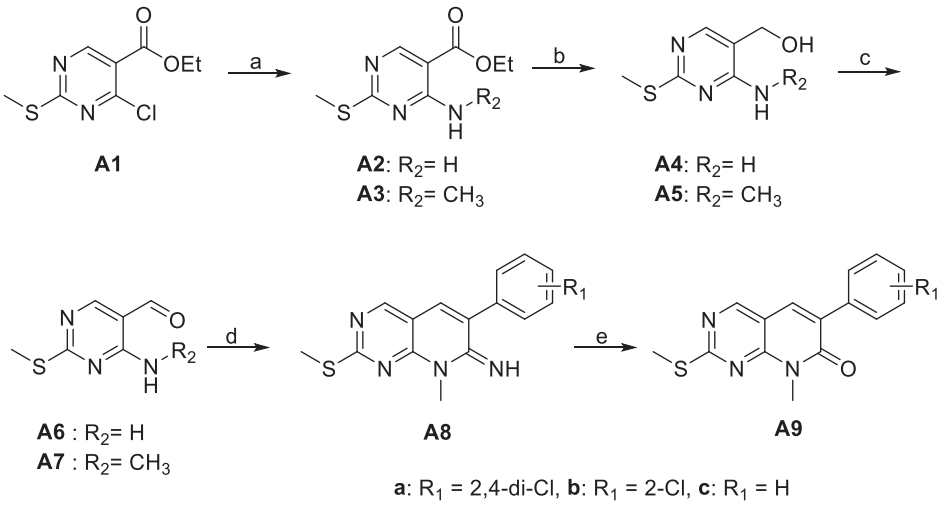

Scheme 1. Synthesis of 2-(methylthio)-6-phenylpyrido[2,3-d]pyrimidin-7-one - intermediates **A9a-c**
*Reagents and conditions: (a) **A2**: NH_4OH, TEA, THF, rt, 2 h (98%), **A3**: CH_3NH_2 (aq), THF, rt, 2 h (85%); (b) LAH, THF, rt, 1.5 h (60–95%); (c) MnO_2, DCM, rt, overnight (83–95%); (d) $PhCH_2CN$, K_2CO_3, DMF, 105 °C, 18 h (54–63%); (e) i) Ac_2O, 139 °C, 30 min, ii) conc. HCl, 100 °C, 5 min (55–65% for two steps).

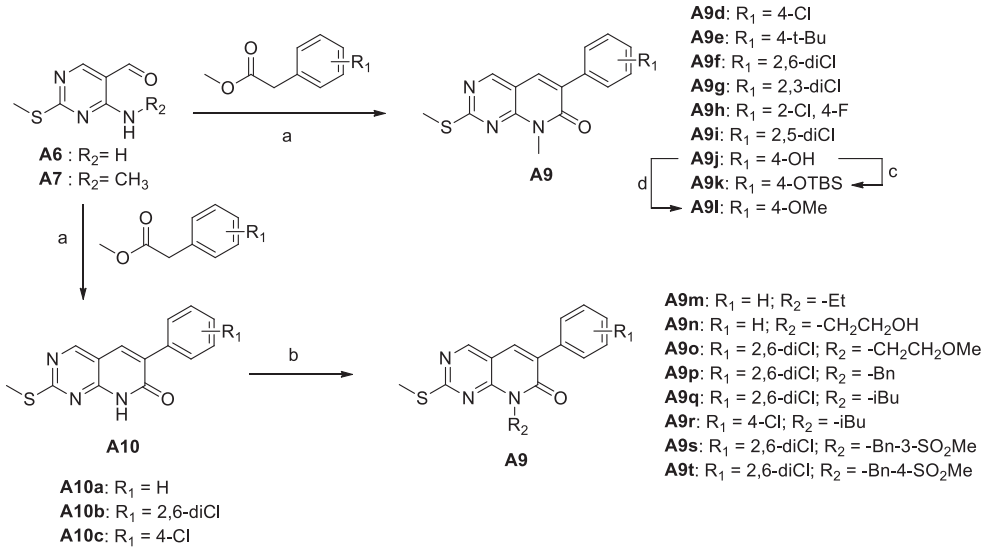

Scheme 2. Synthesis of 2-(methylthio)-6-phenylpyrido[2,3-d]pyrimidin-7-one intermediates **A9d-t**
*Reagents and conditions: (a) KF/Al_2O_3, DMA, rt, 3–4 h (23–60%); (b) R_2I, NaH, DMF, 50 °C, 1 h (28–74%); (c) TBSCl, DMAP, imidazole, DMF, 0 °C to rt, overnight (88%); (d) MeI, K_2CO_3, acetone, reflux, 8 h (95%).

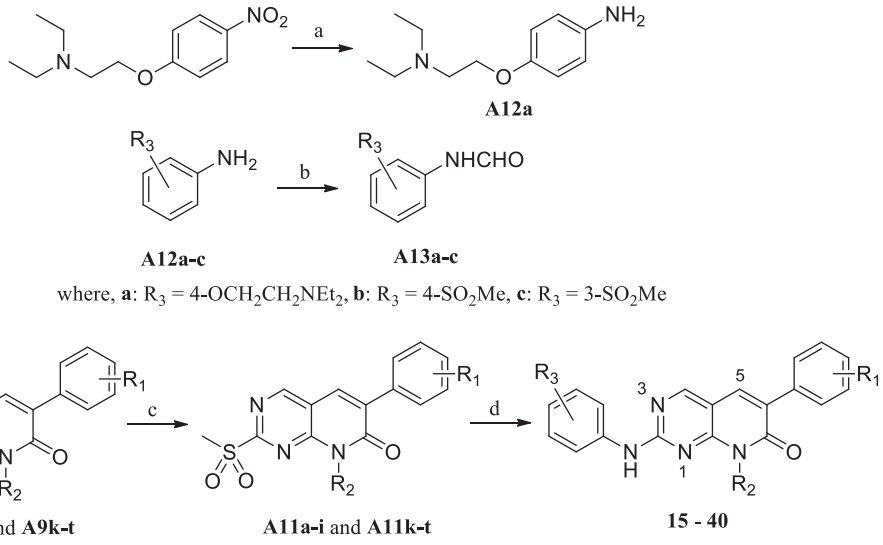

Scheme 3. Synthesis of 6-phenyl-2-(phenylamino)pyrido[2,3-d]pyrimidin-7-ones **15**–**37** and **39**–**40***
*Reagents and conditions: (a) Pd/C (10%), H_2 (1 atm), CH_3OH, rt, overnight (96%); (b) HCO_2H, rt or 60 °C, overnight (79–80%); (c) m-CPBA, DCM, rt, 3–5 h (40–93%); (d) **A13a**, **A13b** or **A13c**, NaH, THF:DMF (1:1), 0 °C to rt, 2.5 h (33–95%). Numbering of the phenylpyrido[2,3-d]pyrimidin-7-one ring system present in compounds **15**–**40** is indicated.

was initially explored. In addition, this region of the kinase appears to be more flexible for RIPK2 since it has been demonstrated to adopt a Glu-out conformation [30], whereas ALK2 seems to be less accommodating of this conformation as evidenced by only DFG-in/Glu-in inhibitors having been reported to date [23,31]. Gratifyingly, **15**, having 2,4-di-Cl substitution, showed improved selectivity towards RIPK2 (Table 1). The absence of the 6-Cl substituent perhaps allow for optimal torsional rotation of the phenyl group favoring RIPK2. However, this compound showed a 4-fold decrease in RIPK2 cellular potency compared to **14**. Removal of the 4-Cl (**16**) resulted in potent RIPK2 enzyme and NOD cell signaling inhibition, but poor ALK2 selectivity. Having only a substituent in the 4-position, including Cl (**17**), *t*-Bu (**18**), OH (**19**) or OMe (**20**), was well tolerated for RIPK2 enzyme inhibition, but resulted in loss of selectivity, cell signaling inhibition or both.

In order to better balance enzyme and cell signaling inhibition with selectivity versus ALK2, the R_2 position on the central heterocycle was explored. Although this group projects towards the glycine-rich loop, the region appears accommodating for larger and more polar substituents. Consequently, an array of groups were introduced (**21**–**28**) into this region of the pyrido[2,3-d]pyrimidine-7-one scaffold. In general, they were well tolerated with regard to maintaining potent RIPK2 and NOD cell signaling inhibition, but offered no selectivity improvement versus ALK2 (Table 2).

Next, the effect of R_3 substituents on RIPK2 selectivity was investigated. This region of the inhibitor is expected to project towards solvent, but also in the vicinity of Ser25. This residue, which is rather unique to RIPK2, has previously been targeted for

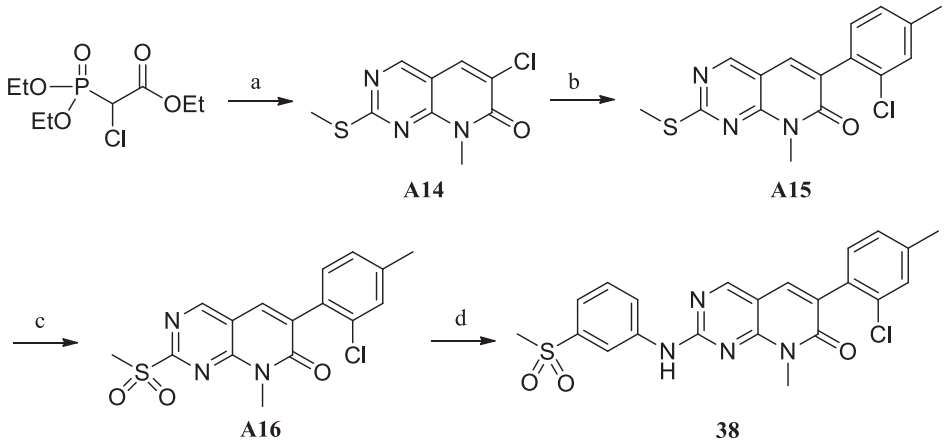

Scheme 4. Synthesis of **38***
*Reagents and conditions: (a) **A7**, NaH, THF, reflux, 2.5 h (42%); (b) 2-Cl-4-MePhB(OH)$_2$, Pd(PPh$_3$)$_4$, Na$_2$CO$_3$, DMF, ACN, 90 °C, 5 h (57%); (c) m-CPBA, DCM, rt, 5 h (68%); (d) **A13c**, NaH, THF, DMF, 0 °C to rt, 2.5 h (75%).

Table 1
RIPK2 and ALK2 kinases, and NOD2 cell (HEKBlue) signaling inhibitory activities of **14**–**20**.

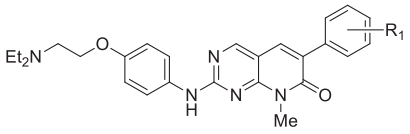

Compound	R_1	Kinase IC_{50} (μM)		RIPK2/NOD2 Cell Assay IC_{50} (μM)
		RIPK2	ALK2	
14	2,6-di-Cl	0.013 ± 0.004	0.021 ± 0.016	0.037 ± 0.004
15	2,4-di-Cl	0.016 ± 0.0036	NI	0.16 ± 0.024
16	2-Cl	0.017 ± 0.008	0.062 ± 0.080	0.004 ± 0.0005
17	4-Cl	0.013 ± 0.0006	2.940 ± 1.633	0.95 ± 0.35
18	4-*t*-Bu	0.105 ± 0.047	NI	1.98 ± 1.73
19	4-OH	0.025 ± 0.014	0.059 ± 0.065	0.005 ± 0.002
20	4-OMe	0.021 ± 0.0016	NI	0.51 ± 0.12

NI: No inhibition observed at 100 μM; IC_{50} values are shown as the mean of two or more determinations ± standard deviation.

engagement as a means to improve selectivity [14]. Incorporation of a hydrogen bond acceptor, such as a sulfone, at either the 3- or 4-positions of the phenyl might provide such an interaction. Indeed, this strategy proved to be effective (Table 3) as it provided 10-fold and 160-fold increase in RIPK2 selectivity versus ALK2 for the 4- (**29**) and 3-methyl sulfone (**30**), respectively. Furthermore, the 3-methyl sulfone **30** retained excellent cellular inhibition. Similar to previous observations, introduction of a substituent in the 4-position for the R_1 group projecting towards the α-C helix, as in **31** and **32**, resulted in loss of cell activity, but not RIPK2 enzyme inhibition. Surprisingly, **33**, which is a mono-substituted phenyl version of **30**, showed further improvement (310-fold) in RIPK2 selectivity versus ALK2 and excellent cellular potency in the HEKBlue assay. Several other substitution arrangements on the phenyl ring projecting towards the α-C helix, including the 3-, 4- and 5-positions (**34**–**40**), were detrimental to cellular activity, despite maintaining potent RIPK2 enzyme inhibition.

In order to further evaluate cellular activities of the pyrido[2,3-d]pyrimidin-7-one series of RIPK2 kinase inhibitors, several representative compounds were assessed in an assay of chemokine CXCL8 positive U2OS/NOD2 cells in response to L18-MDP stimulation [19]. Four potent inhibitors of RIPK2 kinase activity with

Table 2
RIPK2 and ALK2 kinases, and NOD2 cell (HEKBlue) signaling inhibitory activities of **21**–**28**.

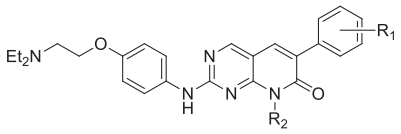

Compound	R_1	R_2	Kinase IC_{50} (μM)		RIPK2/NOD2 Cell Assay IC_{50} (μM)
			RIPK2	ALK2	
21	H	Me	0.0105 ± 0.002	0.284 ± 0.356	0.014 ± 0.004
22	H	Et	~ 30 nM	0.004 ± 0.005	0.015 ± 0.005
23	H	CH_2CH_2OH	~ 30 nM	0.018 ± 0.024	0.27 ± 0.22
24	2,6-di-Cl	CH_2CH_2OMe	0.128 ± 0.001	0.018 ± 0.019	0.013 ± 0.007
25	2,6-di-Cl	CH_2Ph	0.021 ± 0.003	0.008 ± 0.004	0.009 ± 0.003
26	2,6-di-Cl	*i*-Bu	0.005 ± 0.002	0.009 ± 0.005	0.003 ± 0.0005
27	2,6-di-Cl	CH_2Ph-3-SO_2Me	0.025 ± 0.008	0.092 ± 0.005	0.005 ± 0.005
28	2,6-di-Cl	CH_2Ph-4-SO_2Me	0.021 ± 0.007	ND	0.094 ± 0.004

ND: Not determined; IC_{50} values are shown as the mean of two or more determinations ± standard deviation, unless otherwise indicated.

Table 3
RIPK2 and ALK2 kinases, and NOD2 cell (HEKBlue) signaling inhibitory activities of methylsulfones **29**–**40**.

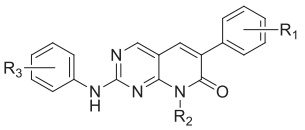

Compound	R_1	R_2	R_3	Kinase IC_{50} (μM)		RIPK2 Cell Assay IC_{50} (μM)
				RIPK2	ALK2	
29	2,6-di-Cl	Me	4-SO_2Me	0.014 ± 0.0001	0.136 ± 0.118	0.136 ± 0.016
30	2,6-di-Cl	Me	3-SO_2Me	0.006 ± 0.0001	0.972 ± 0.510	0.022 ± 0.018
31	4-Cl	Me	3-SO_2Me	0.0146 ± 0.005	NI[a]	NI[b]
32	4-Cl	*i*-Bu	3-SO_2Me	0.0647 ± 0.024	NI[a]	NI[b]
33	2-Cl	Me	3-SO_2Me	0.008 ± 0.004	2.516 ± 2.168	0.020 ± 0.005
34	2,4-diCl	Me	3-SO_2Me	0.027 ± 0.013	NI[a]	0.878 ± 0.23
35	2,3-di-Cl	Me	3-SO_2Me	0.034 ± 0.011	NI[a]	1.23 ± 0.156
36	2-Cl, 4-F	Me	3-SO_2Me	0.017 ± 0.001	NI[a]	0.218 ± 0.049
37	2,5-di-Cl	Me	3-SO_2Me	0.022 ± 0.0007	ND	0.73 ± 0.32
38	2-Cl, 4-Me	Me	3-SO_2Me	0.015 ± 0.002	ND	0.48 ± 0.04
39	4-OH	Me	3-SO_2Me	0.016 ± 0.001	24.80	NI[b]
40	4-OMe	Me	3-SO_2Me	0.011 ± 0.004	NI[a]	NI[b]

NI[a]: No inhibition observed at 100 μM; NI[b]: No inhibition observed at 10 μM; ND: Not determined; IC_{50} values are shown as the mean of two or more determinations ± standard deviation.

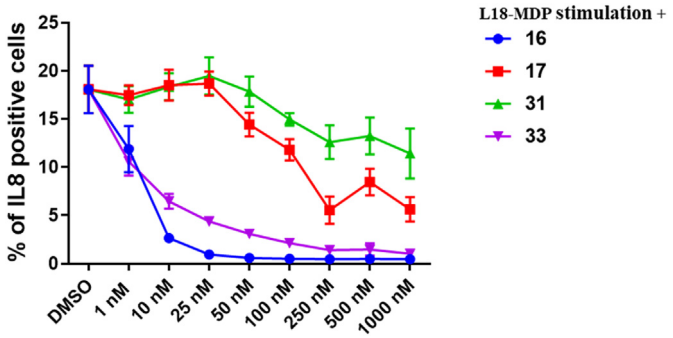

Fig. 3. Intracellular flow cytometry analysis of CXCL8 in U2OS/NOD2 cells treated with L18-MDP (200 ng/mL, 4 h). Percentage of CXCL8 positive cells in the presence of inhibitors **16**, **17**, **31** and **33** at various concentrations versus DMSO control shown. Data points are the average of three experiments.

variable potency in the HEKBlue assay were selected for testing. Compounds **16** and **33** showed potent inhibition of CXCL8 positive cells compared to **17** and **31** (Fig. 3). However, these compounds were inactive in RIPK2 T95W gatekeeper mutant U2OS/NOD2 cells confirming that blocking NF-κB mediated CXCL8 production was mediated through RIPK2 engagement (see supporting information, Figure S1). Compound **33** also demonstrated only marginal activity (IC_{50} > 4 μM) blocking RIPK1- and RIPK3-dependent necroptosis in human U937 monocytes (Figure S2 [32]) suggesting ~3-orders of magnitude difference in potency in inhibiting cellular RIPK2 signaling versus its two most closely related homologues [33].

Molecular docking studies were performed using AutoDock 4.2 (with tools version 1.5.6) software. Inhibitor **14** was docked into the ATP binding site of the kinase domain of RIPK2 using the apo structure (PDB: 5AR2) [30]. The protein was kept rigid, but the ligand was allowed partial flexibility by setting the number of rotatable bonds. The top five poses showed a clustered root mean squared deviation (RMSD) < 2 Å and the binding energy for the top pose was −8.73 kcal/mol (Fig. 4A). Importantly, two hydrogen bonds (both 1.8 Å) involving the ligand NH and N-3 with the backbone of M98 in the hinge were observed. The 2,6-dichlorophenyl projected towards a region between the

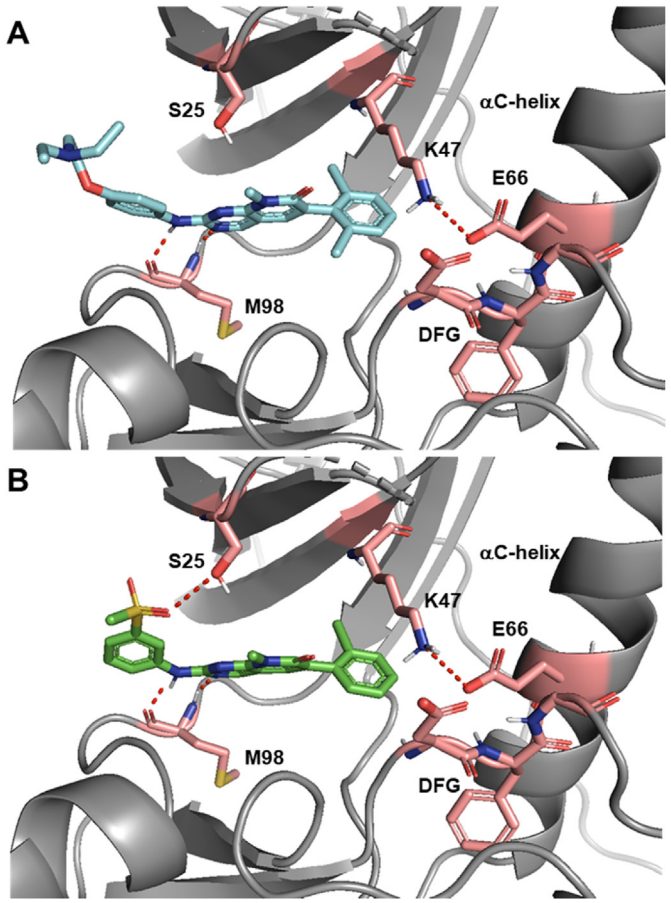

Fig. 4. (**A**) Molecular docking model of **14** (cyan) with RIPK2 (PDB:5AR2). Hydrogen bonding interactions (1.8 Å) between the inhibitor and hinge residue M98, as well as the salt-bridge between K47 and E66 of the αC-helix are shown. Also highlighted is the DFG motif. (**B**) Molecular docking model of **33** (green) with RIPK2 (PDB:5AR2). Hydrogen bonding interaction (3.2 Å) between the inhibitor and S25 is indicated.

gatekeeper and the αC-helix, while the aminoether on the aniline was directed towards the solvent exposed region and the glycine-rich loop.

Based on excellent selectivity versus ALK2, lack of necroptosis inhibition, and potent NOD cell signaling inhibition, **33** was similarly docked with RIPK2 (PDB: 5AR2). The molecular docking model (Fig. 4B, binding energy of −9.07 kcal/mol) resembles the pose of **14** with respect to the hinge interaction and projection of the 2-chlorophenyl towards a region between the gatekeeper and the αC-helix. In addition, the sulfone forms a H-bonding interaction with Ser25 (3.2 Å) in the glycine-rich loop. This model also resembles the RIPK2•**7** co-crystal structure (PDB: 5J7B) [14], except interaction with the backbone of Asp164 in the DFG motif was not observed.

For a previous class of RIPK2 inhibitors (e.g. **12**), we proposed that appropriate occupancy of the region between the gatekeeper and the αC-helix was necessary to achieve NOD cell signaling inhibition, but not required for disruption of RIPK2 kinase activity [18,19]. The pyrido[2,3-d]pyrimidin-7-ones series displayed similar discordance between NOD2 signaling and RIPK2 inhibitory activity with the determinant again being the phenyl directed towards the region between the gatekeeper and the αC-helix. To further explore this observation, three derivatives with different substituents on the phenyl (e.g. **31**, **33** and **34**) demonstrating potent RIPK2 kinase inhibition but an array of potencies for NOD2 signaling inhibition were docked with RIPK2. In all three cases, similar docking poses showed interactions with hinge residue M98 and Ser25, which was consistent with the observed selectivity versus ALK2 (Figure S3A). The phenyl directed towards the region between the gatekeeper and αC-helix was slightly shifted for **31** and **34** possibility due to unfavorable interaction of the 4-Cl with E66 of the αC-helix. In poses where H-bonding to Ser25 was disrupted due to rotation of the phenylsulfone, this shift was even greater (Figure S3B). Overall, only **33** maintains the positioning of the 2-chlorophenyl in the subpocket between the αC-helix and T95 gatekeeper, which is critical for the inhibition of NOD2 signaling [19] independent of H-bonding to Ser25 (Figure S3C). The robustness of the binding provides a possible explanation for the improved inhibition of NOD2 cell signaling by **33** compared to the other two compounds.

Finally, several *in vitro* ADME as well as *in vivo* pharmacokinetic and brain permeability properties of **33** were assessed. The inhibitor demonstrated relatively good stability in mouse liver microsomes ($t_{1/2}$ = 19.7 min; Cl_{int} = = 35 μL/min/mg), aqueous kinetic solubility at pH 7.4 of 0.7 μM, and good permeability (PAMPA $P_{app} = 23.6 \times 10^{-6}$ cm/s). A pharmacokinetic study in female ICR mice (N = 18) following a 10 mg/kg single intraperitoneal administration [formulated with DMSO (5%), Solutol® (10%) and water (85%)] achieved maximum plasma concentration (C_{max}) of 5.7 μM, time to maximum plasma concentration (T_{max}) of 15 min, plasma elimination half-life ($t_{1/2}$) of 3.4 h and clearance (Cl) of 45 mL/min/kg. Brain concentrations of 2.45 μM and 0.32 μM were also observed at 30 min and 2 h post-administration.

4. Conclusions

In conclusion, a new class of pyrido[2,3-d]pyrimidin-7-one based RIPK2 kinase inhibitors was discovered. In addition, optimal substitution of the phenyl group directed towards the region between the gatekeeper and the αC-helix as well as the 3-methyl sulfone on the phenyl ring extending towards the solvent-exposed region with possible engagement of Ser25 in the glycine-rich loop provides increased selectivity versus ALK2 and potent NOD2 cell signaling inhibition. For example, a representative compound **33** demonstrated both potent inhibition of RIPK2 kinase (IC_{50} = 8 ± 4 nM), >300-fold selectivity versus ALK2, as well as blocked HEKBlue NF-κB activation (IC_{50} = 20 ± 5 nM) and L18-MDP stimulated CXCL8 production (at concentrations > 10 nM and was eliminated in RIPK2 T95W mutant U2OS/NOD2 cells). In addition, this compound has *in vitro* ADME and pharmacokinetic characteristics (e.g. C_{max} = 5.7 μM, T_{max} = 15 min, $t_{1/2}$ = 3.4 h and Cl = 45 mL/min/kg following single 10 mg/kg intraperitoneal administration) further supporting use of pyrido[2,3-d]pyrimidin-7-ones (e.g. **33**, a.k.a. **UH15**−**15**) as a new structure class of RIPK2 kinase and NOD cell signaling inhibitors.

5. Experimental section

All reactions were carried out under an argon atmosphere with dry solvents unless otherwise stated. All commercially available chemicals and reagent grade solvents were used directly without further purification unless otherwise specified. Reactions were monitored by thin-layer chromatography (TLC) on Baker-flex® silica gel plates (IB2−F) using UV-light (254 and 365 nm) as a visualizing agent and either an ethanolic solution of phosphomolybdic acid or ninhydrin solution and heat as developing agents. Flash chromatography was conducted on silica gel (230−400 mesh) using Teledyne ISCO CombiFlash® Rf. Melting points were measured using a Thomas Hoover Uni-Melt capillary melting point apparatus. NMR spectra were recorded at room temperature using a JEOL ECA-500 (^{1}H NMR at 400, 500 and 600 MHz and ^{13}C NMR at 100, 125 and 150 MHz) with tetramethylsilane (TMS) as an internal standard. Chemical shifts (δ) are given in parts per million (ppm) with reference to solvent signals [^{1}H NMR: $CDCl_3$ (7.26 ppm), CD_3OD (3.30 ppm), DMSO-d_6 (2.50 ppm); ^{13}C NMR: $CDCl_3$ (77.0 ppm), CD_3OD (49.0 ppm), DMSO-d_6 (39.5 ppm)]. Signal patterns are reported as s (singlet), d (doublet), t (triplet), q (quartet), dd (doublet of doublets), td (triplet of doublets), m (multiplet) and brs (broad singlet). Coupling constants (J) are given in Hz. High-resolution mass spectra (HRMS) were carried out using Agilent 6530 Q-TOF instrument by the mass spectrometry facility at the Department of Chemistry, University of Texas at Austin. Electrospray ionization (ESI) were used as ionization source and the spectra were reported as m/z (relative intensity) for the molecular [M] or $[M + H]^+$ ion species. The purity of the final compounds was determined to be ≥ 95% by analytical high-performance liquid chromatography (HPLC) using binary HPLC pump (Waters) and Kinetex 5 μm C18 100A column (250 × 4.6 mm). UV absorption was monitored at λ = 254 nm. The injection volume was 15 μL. The HPLC gradient of acetonitrile/water (both containing 0.1% trifluoroacetic acid) went from 2:98 to 90:10 with a total run time of 30 min and a flow rate of 1 mL/min.

Ethyl 4-amino-2-(methylthio)pyrimidine-5-carboxylate (A2). To a solution of ethyl 4-chloro-2-(methylthio)pyrimidine-5-carboxylate **(A1)** (100 mg, 0.43 mmol) in dry THF (2 mL) was added triethylamine (0.2 mL, 1.29 mmol) and ammonium hydroxide (0.5 mL). The resulting mixture was stirred at room temperature (rt) for 2 h. After evaporation *in vacuo* to remove THF, the crude mixture was partitioned between water and EtOAc. The organic layer was washed with brine, dried over anhydrous Na_2SO_4, filtered and concentrated. The residue was purified by column chromatography on silica gel (15% EtOAc/hexane) to afford **A2** (90 mg, 98%) as a white solid. ^{1}H NMR (400 MHz, $CDCl_3$) δ 8.65 (s, 1H), 7.81 (s, 1H), 6.05 (s, 1H), 4.29 (q, J = 7.2 Hz, 2H), 2.46 (s, 3H), 1.32 (t, J = 7.1 Hz, 3H). ^{13}C NMR (100 MHz, $CDCl_3$) δ 176.1, 166.4, 161.9, 158.9, 101.1, 61.0, 14.3, 14.1.

Ethyl 4-(methylamino)-2-(methylthio)pyrimidine-5-carboxylate (A3). Aqueous methyl amine (6 mL) was added to the solution of ethyl 4-chloro-2-(methylthio)pyrimidine-5-carboxylate (**A1**) (3.0 g, 12.93 mmol) in dry THF (20 mL) and the mixture was stirred at rt for 2 h. After evaporation *in vacuo* to

remove THF, the crude mixture was then partitioned between H_2O and EtOAc. The organic layer was washed with brine, dried over anhydrous Na_2SO_4, filtered and concentrated. The residue was purified by column chromatography on silica gel (10% EtOAc/hexane) to afford **A3** (2.5 g, 85%) as a white solid. ^{1}H NMR (400 MHz, $CDCl_3$) δ 8.59 (s, 1H), 8.16 (s, 1H), 4.29 (q, J = 7.0 Hz, 2H), 3.06 (d, J = 5.0 Hz, 3H), 2.53 (s, 3H), 1.35 (t, J = 7.1 Hz, 3H). ^{13}C NMR (100 MHz, $CDCl_3$) δ 176.1, 167.1, 160.8, 158.2, 101.0, 60.9, 27.4, 14.3, 14.3.

(4-Amino-2-(methylthio)pyrimidin-5-yl)methanol (A4). A solution of **A2** (450 mg, 2.11 mmol) in THF (2 mL) was added dropwise to the suspension of $LiAlH_4$ (120 mg, 3.16 mmol) in THF (4 mL) at 0 °C and the resulting mixture was then allowed to stir at rt for 30 min. The reaction mixture was cooled at 0 °C and 15% NaOH (0.5 mL) and water (1 mL) was added dropwise. The reaction mixture was then stirred for 1 h, filtered and washed with EtOAc. Evaporation to remove EtOAc *in vacuo* afforded **A4** (220 mg, 61%) as a light-yellow solid, which was used in the next step without purification. ^{1}H NMR (400 MHz, CD_3OD) δ 7.84 (s, 1H), 4.45 (s, 2H), 2.47 (s, 3H). ^{13}C NMR (100 MHz, CD_3OD) δ 170.4, 162.3, 152.6, 111.9, 58.5, 12.6.

(4-(Methylamino)-2-(methylthio)pyrimidin-5-yl)methanol (A5). This compound was synthesized in a similar manner as **A4** to give a pale yellow solid (95% yield). ^{1}H NMR (400 MHz, CD_3OD) δ 7.72 (s, 1H), 4.42 (s, 2H), 3.01 (s, 3H), 2.51 (s, 3H).

4-Amino-2-(methylthio)pyrimidine-5-carbaldehyde (A6). MnO_2 (670 mg, 7.71 mmol) was added to the solution of **A4** (220 mg, 1.28 mmol) in DCM (5 mL) and the resulting mixture was stirred overnight at rt under argon. The reaction mixture was then filtered, concentrated to remove DCM and purified by column chromatography on silica gel (30% EtOAc/hexane) to afford **A6** (180 mg, 83%) as a light yellow solid. ^{1}H NMR (400 MHz, $CDCl_3$) δ 9.77 (s, 1H), 8.41 (s, 1H), 8.19 (s, 1H), 5.81 (s, 1H), 2.54 (s, 3H). ^{13}C NMR (100 MHz, $CDCl_3$) δ 190.7, 177.6, 162.9, 160.4, 109.4, 14.3.

4-(Methylamino)-2-(methylthio)pyrimidine-5-carbaldehyde (A7). This compound was synthesized in a similar manner as **A6** to give a pale yellow solid (77% yield). ^{1}H NMR (400 MHz, $CDCl_3$) δ (ppm) 9.69 (s, 1H), 8.55 (s, 1H), 8.29 (s, 1H), 3.11 (d, J = 5.0 Hz, 3H), 2.56 (s, 3H). ^{13}C NMR (100 MHz, $CDCl_3$) δ 190.2, 177.6, 162.8, 159.5, 109.5, 27.2, 14.4.

General procedure for the preparation of pyrimidin-7(8H)-imines (A8a-c). Exemplified for 6-(2,4-dichlorophenyl)-8-methyl-2-(methylthio)pyrido[2,3-d]pyrimidin-7(8H)-imine (A8a). To a mixture of 4-(methylamino)-2-(methylthio)pyrimidine-5-carbaldehyde (**A7**) (250 mg, 1.37 mmol), 2-(2,4-dichlorophenyl) acetonitrile (381 mg, 2.05 mmol) and K_2CO_3 (944 mg, 6.82 mmol) in a round-bottom flask was added DMF (4 mL) under argon and then the solution was refluxed for 18 h. The reaction mixture was partitioned between water and EtOAc. The organic layer was washed with a brine solution. Evaporation of the organic layer *in vacuo* gave a residue that was purified by column chromatography on silica gel (5% MeOH/DCM) to afford **A8a** as a pale red solid (63% yield). ^{1}H NMR (400 MHz, $CDCl_3$) δ 8.34 (s, 1H), 7.57 (d, J = 2 Hz, 1H), 7.41–7.37 (dd, J = 2.4, 2 Hz, 1H), 7.25–7.23 (m, 1H), 7.05 (s, 1H), 3.79 (s, 3H), 2.63 (s, 3H).

6-(2-Chlorophenyl)-8-methyl-2-(methylthio)pyrido[2,3-d]pyrimidin-7(8H)-imine (A8b). This compound was prepared in the similar manner as **A8a** and used in the next step without purification.

8-Methyl-2-(methylthio)-6-phenylpyrido[2,3-d]pyrimidin-7(8H)-imine (A8c). Light red solid (Yield 54%): ^{1}H NMR (400 MHz, $CDCl_3$) δ 8.32 (s, 1H), 7.50–7.45 (m, 3H), 7.41–7.37 (m, 2H), 7.04 (s, 1H), 3.79 (s, 3H), 2.63 (s, 3H).

General procedure for the preparation of pyrido[2,3-d]pyrimidin-7(8H)-ones (A9a-c). Exemplified for 6-(2,4-dichlorophenyl)-8-methyl-2-(methylthio)pyrido[2,3-d]pyrimidin-7(8H)-one (A9a). A suspension of **A8a** (200 mg, 0.57 mmol) in acetic anhydride (3 mL) was refluxed for 30 min. Evaporation of solvent *in vacuo* gave a residue that was treated with concentrated HCl (2 mL) and refluxed for 5 min. The reaction mixture was then neutralized with saturated solution of $NaHCO_3$ and partitioned between water and EtOAc. The organic layer was washed with brine solution, filtered and concentrated to get a residue that was purified by column chromatography on silica gel (30% EtOAc/Hexane) to afford **A9a** as a pale yellow solid (65% yield). ^{1}H NMR (400 MHz, $CDCl_3$) δ 8.64 (s, 1H), 7.65–7.62 (m, 1H), 7.51 (s, 1H), 7.34–7.29 (m, 2H), 3.82 (s, 3H), 2.66 (s, 3H).

6-(2-Chlorophenyl)-8-methyl-2-(methylthio)pyrido[2,3-d]pyrimidin-7(8H)-one (A9b). Pale yellow solid (61% yield): ^{1}H NMR (400 MHz, $CDCl_3$) δ 8.64 (s, 1H), 7.64 (s, 1H), 7.48–7.46 (m, 1H), 7.36–7.33 (m, 3H), 3.81 (s, 3H), 2.65 (s, 3H). ^{13}C NMR (100 MHz, $CDCl_3$) δ 173.5, 161.8, 156.5, 154.3, 135.0, 134.7, 133.7, 131.6, 131.5, 129.9, 129.9, 126.9, 109.4, 28.5, 14.6.

8-Methyl-2-(methylthio)-6-phenylpyrido[2,3-d]pyrimidin-7(8H)-one (A9c). Yellow solid (55% yield): ^{1}H NMR (500 MHz, $CDCl_3$) δ (ppm) 8.63 (s, 1H), 7.69 (s, 1H), 7.67–7.63 (m, 2H), 7.45–7.36 (m, 3H), 3.81 (s, 3H), 2.64 (s, 3H). ^{13}C NMR (125 MHz, $CDCl_3$) δ 172.8, 162.4, 156.3, 153.9, 135.6, 132.8, 132.6, 128.9, 128.7, 128.4, 109.9, 28.5, 14.6.

General procedure for the preparation of pyrido[2,3-d]pyrimidin-7(8H)-ones (A9d-j) and (A10a-c). Exemplified for 6-(4-chlorophenyl)-8-methyl-2-(methylthio)pyrido[2,3-d]pyrimidin-7(8H)-one (A9d). KF/Al_2O_3 (70 mg, 40 wt %) was added to a stirring solution of **A7** (15 mg, 0.08 mmol) and methyl 2-(4-chlorophenyl)acetate (23 mg, 0.12 mmol) in dry DMA (1.5 mL). The mixture was stirred at rt for 3 h under argon. The reaction mixture was then filtered through Celite and the residual solid was washed with DCM. The filtrate was concentrated and the residue was purified by column chromatography over silica gel (15% EtOAc/hexane) to afford **A9d** as a light-yellow solid (58% yield). ^{1}H NMR (500 MHz, $CDCl_3$) δ 8.65 (s, 1H), 7.67 (s, 1H), 7.61 (d, J = 8.5 Hz, 2H), 7.40 (d, J = 8.5 Hz, 2H), 3.81 (s, 3H), 2.65 (s, 3H). ^{13}C NMR (125 MHz, $CDCl_3$) δ 173.2, 162.2, 156.4, 153.9, 134.7, 134.0, 132.7, 131.5, 130.2, 128.6, 109.7, 28.5, 14.6.

6-(4-(*Tert*-butyl)phenyl)-8-methyl-2-(methylthio)pyrido[2,3-d]pyrimidin-7(8H)-one (A9e). Yellow solid (41% yield): ^{1}H NMR (400 MHz, $CDCl_3$) δ 8.64 (s, 1H), 7.68 (s, 1H), 7.61 (d, J = 6 Hz, 2H), 7.46 (d, J = 7.6 Hz, 2H), 3.81 (s, 3H), 2.64 (s, 3H), 1.35 (s, 9H). ^{13}C NMR (100 MHz, $CDCl_3$) δ 172.6, 162.5, 156.1, 153.9, 151.8, 132.7, 132.7, 132.1, 128.6, 125.4, 110.0, 34.8, 31.4, 28.5, 14.6.

6-(2,6-Dichlorophenyl)-8-methyl-2-(methylthio)pyrido[2,3-d]pyrimidin-7(8H)-one (A9f). White solid (30% yield): ^{1}H NMR (400 MHz, $CDCl_3$) δ (ppm) 8.67 (s, 1H), 7.61 (s, 1H), 7.42 (d, J = 7.8 Hz, 2H), 7.33–7.26 (m, 1H), 3.84 (s, 3H), 2.67 (s, 3H). ^{13}C NMR (100 MHz, $CDCl_3$) δ 173.8, 161.0, 156.6, 154.5, 136.0, 135.5, 133.7, 130.3, 129.5, 128.2, 109.2, 28.5, 14.6.

6-(2,3-Dichlorophenyl)-8-methyl-2-(methylthio)pyrido[2,3-d]pyrimidin-7(8H)-one (A9g). White solid (38% yield): ^{1}H NMR (500 MHz, $CDCl_3$) δ 8.65 (s, 1H), 7.64 (s, 1H), 7.52 (dd, J = 7.5, 2 Hz, 1H), 7.30–7.24 (m, 2H), 3.82 (s, 3H), 2.67 (s, 3H).

6-(2-Chloro-4-fluorophenyl)-8-methyl-2-(methylthio)pyrido[2,3-d]pyrimidin-7(8H)-one (A9h). White solid (35% yield): ^{1}H NMR (400 MHz, $CDCl_3$) δ 8.63 (s, 1H), 7.64 (s, 1H), 7.35–7.30 (m, 1H), 7.24–7.15 (m, 1H), 7.04 (td, J = 8.4, 2.8 Hz, 1H), 3.80 (s, 3H), 2.64 (s, 3H). ^{13}C NMR (150 MHz, $CDCl_3$) δ 173.6, 163.3, 161.8, 161.7, 156.5, 154.3, 135.3, 134.7, 134.6, 132.6, 132.6, 130.8, 130.5, 117.4, 117.2, 114.3, 114.1, 109.3, 28.5, 14.6.

6-(2,5-Dichlorophenyl)-8-methyl-2-(methylthio)pyrido[2,3-d]pyrimidin-7(8H)-one (A9i). White solid (23% yield): ^{1}H NMR (400 MHz, $CDCl_3$) δ 8.65 (s, 1H), 7.66 (s, 1H), 7.43–7.31 (m, 3H), 3.82

(s, 3H), 2.66 (s, 3H).

6-(4-Hydroxyphenyl)-8-methyl-2-(methylthio)pyrido[2,3-d] pyrimidin-7(8H)-one (A9j). Light yellow solid (55% yield): ^{1}H NMR (400 MHz, DMSO-d_6) δ 9.68 (s, 1H), 8.87 (s, 1H), 7.99 (s, 1H), 7.54 (d, J = 8.8 Hz, 2H), 6.81 (d, J = 8 Hz, 2H), 3.64 (s, 3H), 2.59 (s, 3H).

6-(4-((*Tert*-butyldimethylsilyl)oxy)phenyl)-8-methyl-2-(methylthio)pyrido[2,3-d]pyrimidin-7(8H)-one (A9k). To a solution of **A9j** (160 mg, 0.53 mmol) in dry DCM (3 mL) were added a catalytic amount of DMAP (3 mg) and imidazole (109 mg, 1.60 mmol). TBDMSCl (121 mg, 0.80 mmol) was then added to the mixture at 0 °C. The resulting mixture was stirred at rt for 4 h. Evaporation of DCM *in vacuo* gave a crude mixture that was portioned between water and DCM. The organic layer was then washed with brine, dried over anhydrous Na_2SO_4, filtered and concentrated. The residue was purified by column chromatography on silica gel (5% EtOAc/DCM) to afford **A9k** as light yellow solid (88% yield). ^{1}H NMR (600 MHz, $CDCl_3$) δ 8.64 (s, 1H), 7.66 (s, 1H), 7.57 (d, J = 8.4 Hz, 2H), 6.89 (d, J = 7.8 Hz, 2H), 3.81 (s, 3H), 2.65 (s, 3H), 0.99 (s, 9H), 0.22 (s, 6H).

6-(4-Methoxyphenyl)-8-methyl-2-(methylthio)pyrido[2,3-d] pyrimidin-7(8H)-one (A9l). Anhydrous K_2CO_3 was added to the solution of **A9j** (20 mg, 0.06 mmol) in dry acetone (2 mL). Iodomethane (10 μL, 0.10 mmol) was added to the mixture and the contents were refluxed for 8 h. The reaction mixture was allowed to cool to rt and then partitioned between water and EtOAc. The organic layer was washed with brine solution. Evaporation to remove EtOAc *in vacuo* gave a residue that was purified by column chromatography on silica gel (50% EtOAc/Hex) to afford **A9l** (20 mg, 95%) as light yellow solid. ^{1}H NMR (400 MHz, $CDCl_3$) δ 8.64 (s, 1H), 7.65–7.62 (m, 3H), 6.96 (d, J = 8.8 Hz, 2H), 3.85 (s, 3H), 3.81 (s, 3H), 2.65 (s, 3H). ^{13}C NMR (100 MHz, $CDCl_3$) δ 172.4, 162.6, 160.0, 156.0, 153.8, 132.4, 131.4, 130.2, 128.0, 113.8, 110.1, 55.5, 28.5, 14.6.

2-(Methylthio)-6-phenylpyrido[2,3-d]pyrimidin-7(8H)-one (A10a). White solid (51% yield): ^{1}H NMR (500 MHz, $CDCl_3$) δ 9.66 (s, 1H), 8.70 (s, 1H), 7.77 (s, 1H), 7.70 (d, J = 7.5 Hz, 2H), 7.47–7.39 (m, 3H), 2.62 (s, 3H). ^{13}C NMR (125 MHz, $CDCl_3$) δ 173.6, 162.3, 156.0, 152.3, 134.7, 134.0, 133.6, 129.0, 128.8, 128.5, 109.6, 14.5.

6-(2,6-Dichlorophenyl)-2-(methylthio)pyrido[2,3-d]pyrimidin-7(8H)-one (A10b). Light yellow solid (28% yield): ^{1}H NMR (400 MHz, $CDCl_3$) δ (ppm) 9.81 (s, 1H), 8.70 (s, 1H), 7.65 (s, 1H), 7.41 (d, J = 8.4 Hz, 2H), 7.30 (dd, J = 8.7, 7.8 Hz, 1H), 2.60 (s, 3H). ^{13}C NMR (100 MHz, $CDCl_3$) δ 174.5, 160.9, 156.4, 153.9, 137.7, 135.6, 132.9, 130.5, 130.3, 128.2, 108.8, 14.5.

6-(4-Chlorophenyl)-2-(methylthio)pyrido[2,3-d]pyrimidin-7(8H)-one (A10c). White solid (40% yield): ^{1}H NMR (400 MHz, $CDCl_3$) δ 9.54 (s, 1H), 8.71 (s, 1H), 7.77 (s, 1H), 7.66 (d, J = 8.8 Hz, 2H), 7.42 (d, J = 8.8 Hz, 2H), 2.62 (s, 3H). ^{13}C NMR (100 MHz, $CDCl_3$) δ 173.9, 161.9, 156.1, 153.3, 135.0, 134.1, 133.1, 132.3, 130.1, 128.7, 109.4, 14.5.

General procedure for the preparation of pyrido[2,3-d]pyrimidin-7(8H)-ones (A9m-t). Exemplified for 8-ethyl-2-(methylthio)-6-phenylpyrido[2,3-d]pyrimidin-7(8H)-one (A9m). Sodium hydride (2.67 mg, 0.11 mmol) was added to the solution of **A10a** (20 mg, 0.07 mmol) in dry DMF (1.5 mL). Ethyl iodide (50 μL, 0.11 mmol) was added to the mixture and then the reaction vessel was heated at 50 °C for 1h. The reaction mixture was partitioned between water and EtOAc and the organic layer was washed with brine solution. Evaporation to remove EtOAc *in vacuo* gave a residue that was purified by column chromatography on silica gel (50% EtOAc/Hex) to afford **A9m** (25 mg, 74%) as a colorless liquid. ^{1}H NMR (400 MHz, $CDCl_3$) δ 8.66 (s, 1H), 7.71–7.65 (m, 3H), 7.47–7.36 (m, 3H), 4.56 (q, J = 7.2 Hz, 2H), 2.65 (s, 3H), 1.37 (t, J = 7.1 Hz, 3H). ^{13}C NMR (100 MHz, $CDCl_3$) δ 172.8, 161.8, 156.4, 153.4, 135.6, 133.0, 132.6, 129.0, 128.7, 128.4, 109.9, 29.8, 14.5, 13.1.

8-(2-Hydroxyethyl)-2-(methylthio)-6-phenylpyrido[2,3-d] pyrimidin-7(8H)-one (A9n). Pale yellow viscous liquid (48% yield): ^{1}H NMR (400 MHz, $CDCl_3$) δ 8.61 (s, 1H), 7.67 (s, 1H), 7.54 (d, J = 8 Hz, 2H), 7.39–7.31 (m, 3H), 4.63 (t, J = 6 Hz, 2H), 3.88 (t, J = 6 Hz, 2H), 2.56 (s, 3H). ^{13}C NMR (100 MHz, $CDCl_3$) δ 172.9, 163.0, 156.5, 153.7, 135.3, 133.4, 132.9, 128.8, 128.8, 128.4, 110.0, 59.9, 43.6, 14.4.

6-(2,6-Dichlorophenyl)-8-(2-methoxyethyl)-2-(methylthio) pyrido[2,3-d]pyrimidin-7(8H)-one (A9o). Colorless liquid (44% yield): ^{1}H NMR (400 MHz, $CDCl_3$) δ 8.67 (s, 1H), 7.62 (s, 1H), 7.41 (d, J = 7.8 Hz, 2H), 7.34–7.25 (m, 1H), 4.74 (t, J = 6.2 Hz, 2H), 3.78 (t, J = 6.2 Hz, 2H), 3.39 (s, 3H), 2.65 (s, 3H). ^{13}C NMR (100 MHz, $CDCl_3$) δ 173.7, 160.7, 156.7, 154.4, 136.2, 135.5, 133.7, 130.2, 129.6, 128.2, 109.3, 69.0, 58.9, 40.3, 14.6.

8-Benzyl-6-(2,6-dichlorophenyl)-2-(methylthio)pyrido[2,3-d]pyrimidin-7(8H)-one (A9p). White semisolid (29% yield): ^{1}H NMR (400 MHz, $CDCl_3$) δ 8.65 (s, 1H), 7.61 (s, 1H), 7.47 (d, J = 6.9 Hz, 2H), 7.41 (d, J = 8.2 Hz, 2H), 7.32–7.22 (m, 4H), 5.70 (s, 2H), 2.61 (s, 3H). ^{13}C NMR (100 MHz, $CDCl_3$) δ 173.9, 160.9, 156.7, 154.2, 136.8, 136.3, 135.5, 133.7, 130.3, 129.8, 128.9, 128.6, 128.6, 128.2, 127.6, 109.4, 44.7, 14.7.

6-(2,6-Dichlorophenyl)-8-isobutyl-2-(methylthio)pyrido[2,3-d]pyrimidin-7(8H)-one (A9q). White solid (28% yield): ^{1}H NMR (400 MHz, $CDCl_3$) δ (ppm) 8.66 (s, 1H), 7.60 (s, 1H), 7.41 (d, J = 8 Hz, 2H), 7.29 (t, J = 8, 7.2 Hz, 1H), 4.36 (d, J = 7.6 Hz, 2H), 2.65 (s, 3H), 2.40–2.30 (sep, J = 6.8, 7.2 Hz, 1H), 0.98 (d, J = 6.9 Hz, 6H). ^{13}C NMR (100 MHz, $CDCl_3$) δ 173.5, 161.0, 156.7, 154.5, 135.9, 135.5, 133.9, 130.2, 129.8, 128.1, 109.1, 48.4, 27.6, 20.4, 14.6.

6-(4-Chlorophenyl)-8-isobutyl-2-(methylthio)pyrido[2,3-d]pyrimidin-7(8H)-one (A9r). Yellow solid (73% yield): ^{1}H NMR (400 MHz, $CDCl_3$) δ 8.66 (s, 1H), 7.70 (s, 1H), 7.63 (d, J = 8.8 Hz, 2H), 7.41 (d, J = 8.8 Hz, 2H), 4.36 (d, J = 7.3 Hz, 2H), 2.64 (s, 3H), 2.33 (sep, J = 7.2, 6.8 Hz, 1H), 0.98 (d, J = 6.8 Hz, 6H).

6-(2,6-Dichlorophenyl)-8-(3-(methylsulfonyl)benzyl)-2-(methylthio)pyrido[2,3-d]pyrimidin-7(8H)-one (A9s). Light yellow solid (36% yield): ^{1}H NMR (400 MHz, $CDCl_3$) δ 8.69 (s, 1H), 8.08 (s, 1H), 7.84 (d, J = 8 Hz, 1H), 7.75 (d, J = 8 Hz, 1H), 7.65 (s, 1H), 7.51 (t, J = 7.8 Hz, 1H), 7.43 (d, J = 8 Hz, 2H), 7.32–7.28 (m, 1H), 5.76 (s, 2H), 3.03 (s, 3H), 2.63 (s, 3H).

6-(2,6-Dichlorophenyl)-8-(4-(methylsulfonyl)benzyl)-2-(methylthio)pyrido[2,3-d]pyrimidin-7(8H)-one (A9t). Pale yellow solid (53% yield): ^{1}H NMR (400 MHz, $CDCl_3$) δ 8.70 (s, 1H), 7.87 (d, J = 8.4 Hz, 2H), 7.67–7.61 (m, 3H), 7.42 (d, J = 8 Hz, 2H), 7.32–7.28 (m, 1H), 5.76 (s, 2H), 3.02 (s, 3H), 2.58 (s, 3H).

4-(2-(Diethylamino)ethoxy)aniline (A12a). To a solution of N,N-diethyl-2-(4-nitrophenoxy)ethanamine (490 mg, 2.06 mmol) in methanol (10 mL) was added 10% Pd/C (125 mg). The reaction was stirred in the presence of H_2 gas (1 atm) for 4 h. The reaction mixture was then filtered through Celite and concentrated to afford **A12a** as a brown viscous liquid (96% yield). ^{1}H NMR (400 MHz, $CDCl_3$) δ 6.75–6.73 (m, 2H), 6.64–6.62 (m, 2H), 3.98 (t, J = 6.4 Hz, 2H), 2.84 (t, J = 6.4 Hz, 2H), 2.63 (q, J = 7.2 Hz, 4H), 1.06 (t, J = 7.2 Hz, 6H). ^{13}C NMR (100 MHz, $CDCl_3$) δ 152.1, 140.0, 116.5, 115.7, 67.0, 51.9, 47.8, 11.8.

General procedure for the preparation of N-phenylformamides A13a-c. Exemplified for N-(4-(2-(diethylamino) ethoxy)phenyl)formamide (A13a). Formic acid (1 mL) was added to **A12a** (100 mg, 0.48 mmol) in a round-bottom flask containing molecular sieves (4 Å, 8–12 mesh)). The reaction mixture was heated at 60 °C for 6 h and then partitioned between a saturated solution of $NaHCO_3$ and EtOAc. The organic layer was washed with brine solution and concentrated to give **A13a** (79% yield) as a brown viscous liquid which was used without purification in the next step.

N-(4-(Methylsulfonyl)phenyl)formamide (A13b). This compound was prepared in a similar manner as **A13a** and used in the next step without purification.

N-(3-(Methylsulfonyl)phenyl)formamide (A13c). White solid (80% yield): ^{1}H NMR (400 MHz, DMSO-d_6) δ 10.64 (s, 1H), 8.40 (s, 1H), 8.28 (s, 1H), 7.89–7.86 (m, 1H), 7.67–7.63 (m, 2H), 3.24 (s, 3H). ^{13}C NMR (100 MHz, DMSO-d_6) δ 160.7, 141.9, 139.4, 130.8, 124.1, 122.5, 117.5, 44.1.

General Procedure for the preparation of 2-(methylsulfonyl) pyrido[2,3-d]pyrimidin-7(8H)-ones (A11a-i) and (A11k-t). Exemplified for 6-(2,4-dichlorophenyl)-8-methyl-2-(methylsulfonyl)pyrido[2,3-d]pyrimidin-7(8H)-one (A11a). m-CPBA (85 mg, 55%) was added to the solution of **A9a** (38 mg, 0.108 mmol) in DCM (2 mL). The solution was stirred for 3 h. The reaction mixture was then partitioned between water and DCM and the organic layer was washed with brine, filtered and concentrated. The residue was purified by column chromatography using silica gel (40% EtOAc/Hexane) to get **A11a** as a white solid (63% yield). ^{1}H NMR (400 MHz, $CDCl_3$) δ 9.01 (s, 1H), 7.82 (s, 1H), 7.53 (d, J = 1.8 Hz, 1H), 7.36 (dd, J = 8.2, 2.3 Hz, 1H), 7.31 (d, J = 8.2 Hz, 1H), 3.89 (s, 3H), 3.43 (s, 3H). ^{13}C NMR (100 MHz, $CDCl_3$) δ 164.7, 161.0, 157.4, 155.2, 136.0, 135.4, 134.3, 134.0, 132.1, 132.0, 131.0, 127.4, 114.9, 39.3, 29.4.

6-(2-Chlorophenyl)-8-methyl-2-(methylsulfonyl)pyrido[2,3-d]pyrimidin-7(8H)-one (A11b). White solid (45% yield): ^{1}H NMR (400 MHz, $CDCl_3$) δ 9.00 (s, 1H), 7.82 (s, 1H), 7.48 (d, J = 7.2 Hz, 1H), 7.42–7.32 (m, 3H), 3.87 (s, 3H), 3.42 (s, 3H). ^{13}C NMR (100 MHz, $CDCl_3$) δ 164.5, 161.2, 157.3, 155.1, 136.5, 133.8, 133.7, 133.4, 131.2, 130.6, 130.0, 127.0, 115.0, 39.4, 29.3.

8-Methyl-2-(methylsulfonyl)-6-phenylpyrido[2,3-d]pyrimidin-7(8H)-one (A11c). Light yellow solid (54% yield): ^{1}H NMR (400 MHz, $CDCl_3$) δ 9.00 (s, 1H), 7.85 (s, 1H), 7.70–7.66 (m, 2H), 7.49–7.44 (m, 3H), 3.88 (s, 3H), 3.42 (s, 3H). ^{13}C NMR (100 MHz, $CDCl_3$) δ 164.0, 161.9, 156.9, 154.6, 137.6, 134.5, 131.15, 129.7, 129.0, 128.6, 115.6, 39.3, 29.3.

6-(4-Chlorophenyl)-8-methyl-2-(methylsulfonyl)pyrido[2,3-d]pyrimidin-7(8H)-one (A11d). White solid (72% yield): ^{1}H NMR (400 MHz, $CDCl_3$) δ 9.01 (s, 1H), 7.86 (s, 1H), 7.652 (d, J = 8.8 Hz, 2H), 7.445 (d, J = 8.8 Hz, 2H), 3.89 (s, 3H), 3.43 (s, 3H). ^{13}C NMR (100 MHz, $CDCl_3$) δ 164.2, 161.6, 157.0, 154.7, 136.4, 135.9, 132.9, 131.2, 130.3, 128.9, 115.4, 39.3, 29.4.

6-(4-(*Tert*-butyl)phenyl)-8-methyl-2-(methylsulfonyl)pyrido[2,3-d]pyrimidin-7(8H)-one (A11e). White solid (81% yield): ^{1}H NMR (400 MHz, $CDCl_3$) δ 8.98 (s, 1H), 7.84 (s, 1H), 7.63 (d, J = 8.8 Hz, 2H), 7.47 (d, J = 8 Hz, 2H), 3.86 (s, 3H), 3.40 (s, 3H), 1.34 (s, 9H). ^{13}C NMR (100 MHz, $CDCl_3$) δ 163.8, 162.0, 156.8, 154.5, 153.0, 137.4, 131.7, 130.6, 128.7, 125.6, 115.7, 39.3, 34.9, 31.3, 29.3.

6-(2,6-Dichlorophenyl)-8-methyl-2-(methylsulfonyl)pyrido[2,3-d]pyrimidin-7(8H)-one (A11f). White solid (93% yield): ^{1}H NMR (600 MHz, $CDCl_3$) δ 9.03 (s, 1H), 7.77 (s, 1H), 7.45 (d, J = 7.8 Hz, 2H), 7.35 (t, J = 7.8, 9 Hz, 1H), 3.91 (s, 3H), 3.44 (s, 3H).

6-(2,3-Dichlorophenyl)-8-methyl-2-(methylsulfonyl)pyrido[2,3-d]pyrimidin-7(8H)-one (A11g). Light yellow solid (65% yield): ^{1}H NMR (400 MHz, $CDCl_3$) δ 9.02 (s, 1H), 7.82 (s, 1H), 7.57 (dd, J = 8, 2 Hz, 1H), 7.34–7.25 (m, 2H), 3.90 (s, 3H), 3.44 (s, 3H). ^{13}C NMR (100 MHz, $CDCl_3$) δ 164.7, 160.9, 157.4, 155.2, 136.4, 135.8, 133.9, 133.7, 132.1, 131.4, 129.2, 127.6, 114.9, 39.3, 29.4.

6-(2-Chloro-4-fluorophenyl)-8-methyl-2-(methylsulfonyl) pyrido[2,3-d]pyrimidin-7(8H)-one (A11h). White solid (40% yield): ^{1}H NMR (400 MHz, $CDCl_3$) δ 9.02 (s, 1H), 7.83 (s, 1H), 7.37 (dd, J = 14, 6.6 Hz, 1H), 7.29–7.26 (m, 1H), 7.11 (td, J = 8, 2.4 Hz, 1H), 3.90 (s, 3H), 3.44 (s, 3H). ^{13}C NMR (150 MHz, $CDCl_3$) δ 164.7, 163.7, 162.0, 161.2, 157.3, 155.1, 135.5, 134.6, 134.5, 134.0, 132.5, 132.4, 129.7, 117.7, 117.5, 114.9, 114.5, 114.4, 39.3, 29.4.

6-(2,5-Dichlorophenyl)-8-methyl-2-(methylsulfonyl)pyrido[2,3-d]pyrimidin-7(8H)-one (A11i). White solid (75% yield): ^{1}H NMR (400 MHz, $CDCl_3$) δ 9.02 (s, 1H), 7.83 (s, 1H), 7.46–7.47 (m, 1H), 7.39–7.36 (m, 2H), 3.89 (s, 3H), 3.44 (s, 3H). ^{13}C NMR (100 MHz, $CDCl_3$) δ 164.8, 160.8, 157.4, 155.2, 135.3, 135.0, 134.1, 132.9, 131.9, 131.2, 131.1, 130.6, 114.8, 39.3, 29.4.

6-(4-((*Tert*-butyldimethylsilyl)oxy)phenyl)-8-methyl-2-(methylsulfonyl)pyrido[2,3-d]pyrimidin-7(8H)-one (A11k). Light yellow solid (64% yield): ^{1}H NMR (600 MHz, $CDCl_3$) δ 8.96 (s, 1H), 7.80 (s, 1H), 7.60 (d, J = 8.4 Hz, 2H), 6.88 (d, J = 8.4 Hz, 2H), 3.85 (s, 3H), 3.39 (s, 3H), 0.98 (s, 9H), 0.21 (s, 6H). ^{13}C NMR (150 MHz, $CDCl_3$) δ 163.6, 162.0, 157.2, 156.6, 154.3, 136.9, 130.4, 129.9, 127.5, 120.2, 115.7, 39.3, 29.2, 25.7, 18.3.

6-(4-Methoxyphenyl)-8-methyl-2-(methylsulfonyl)pyrido[2,3-d]pyrimidin-7(8H)-one (A11l). Yellow solid (97% yield): ^{1}H NMR (400 MHz, $CDCl_3$) δ 8.98 (s, 1H), 7.80 (s, 1H), 7.68 (d, J = 8.8 Hz, 2H), 6.98 (d, J = 8.8 Hz, 2H), 3.88 (s, 3H), 3.86 (s, 3H), 3.42 (s, 3H).

8-Ethyl-2-(methylsulfonyl)-6-phenylpyrido[2,3-d]pyrimidin-7(8H)-one (A11m). White solid (55% yield): ^{1}H NMR (400 MHz, $CDCl_3$) δ 9.01 (s, 1H), 7.85 (s, 1H), 7.72–7.67 (m, 2H), 7.52–7.44 (m, 3H), 4.60 (q, J = 7.0 Hz, 2H), 3.42 (s, 3H), 1.40 (t, J = 7.1 Hz, 3H).

8-(2-Hydroxyethyl)-2-(methylsulfonyl)-6-phenylpyrido[2,3-d]pyrimidin-7(8H)-one (A11n). Light yellow solid (81% yield), which was used without purification in next step.

6-(2,6-Dichlorophenyl)-8-(2-methoxyethyl)-2-(methylsulfonyl)pyrido[2,3-d]pyrimidin-7(8H)-one (A11o). White solid (58% yield): ^{1}H NMR (400 MHz, $CDCl_3$) δ 9.02 (s, 1H), 7.78 (s, 1H), 7.43 (d, J = 8.2 Hz, 2H), 7.33 (dd, J = 8.8, 7.2 Hz, 1H), 4.79 (t, J = 5.6 Hz, 2H), 3.80 (t, J = 5.6 Hz, 2H), 3.41 (s, 3H), 3.36 (s, 3H). ^{13}C NMR (100 MHz, $CDCl_3$) δ 164.6, 160.2, 157.6, 155.4, 135.1, 134.6, 132.7, 130.9, 128.3, 114.9, 69.1, 59.0, 41.2, 39.4.

8-Benzyl-6-(2,6-dichlorophenyl)-2-(methylsulfonyl)pyrido[2,3-d]pyrimidin-7(8H)-one (A11p). White solid (61% yield): ^{1}H NMR (400 MHz, $CDCl_3$) δ 9.01 (s, 1H), 7.78 (s, 1H), 7.59 (d, J = 7.6 Hz, 2H), 7.45 (d, J = 8 Hz, 2H), 7.39–7.24 (m, 4H), 5.73 (s, 2H), 3.33 (s, 3H). ^{13}C NMR (100 MHz, $CDCl_3$) δ 164.6, 160.4, 157.6, 154.9, 135.8, 135.1, 134.9, 132.7, 130.9, 129.3, 128.7, 128.3, 128.2, 115.0, 45.5, 39.5.

6-(2,6-Dichlorophenyl)-8-isobutyl-2-(methylsulfonyl)pyrido[2,3-d]pyrimidin-7(8H)-one (A11q). White solid (87% yield): ^{1}H NMR (400 MHz, $CDCl_3$) δ 9.03 (s, 1H), 7.77 (s, 1H), 7.43 (d, J = 7.6 Hz, 2H), 7.33 (dd, J = 9.0, 7.4 Hz, 1H), 4.40 (d, J = 7.3 Hz, 2H), 3.41 (s, 3H), 2.37–2.27 (sep, J = 6.8, 7.2 Hz, 1H), 0.98 (d, J = 6.9 Hz, 6H). ^{13}C NMR (100 MHz, $CDCl_3$) δ 164.7, 160.4, 157.7, 155.2, 135.0, 134.8, 134.7, 132.9, 130.8, 128.3, 114.8, 49.1, 39.3, 27.6, 20.3.

6-(4-Chlorophenyl)-8-isobutyl-2-(methylsulfonyl)pyrido[2,3-d]pyrimidin-7(8H)-one (A11r). Light brown solid (66% yield), which was used without purification in next step.

6-(2,6-Dichlorophenyl)-2-(methylsulfonyl)-8-(3-(methylsulfonyl)benzyl)pyrido[2,3-d]pyrimidin-7(8H)-one (A11s). White powder (79% yield): ^{1}H NMR (500 MHz, $CDCl_3$) δ 9.03 (s, 1H), 8.25 (s, 1H), 7.91 (d, J = 8 Hz, 1H), 7.86 (d, J = 8 Hz, 1H), 7.81 (s, 1H), 7.52 (t, J = 7.5 Hz, 1H), 7.46 (d, J = 7.5 Hz, 2H), 7.38–7.33 (m, 1H), 5.79 (s, 2H), 3.39 (s, 3H), 3.09 (s, 3H).

6-(2,6-Dichlorophenyl)-2-(methylsulfonyl)-8-(4-(methylsulfonyl)benzyl)pyrido[2,3-d]pyrimidin-7(8H)-one (A11t). White powder (72% yield): ^{1}H NMR (500 MHz, $CDCl_3$) δ 9.03 (s, 1H), 7.89–7.81 (m, 5H), 7.46 (d, J = 8 Hz, 2H), 7.38–7.35 (m, 1H), 3.37 (s, 3H), 3.01 (s, 3H).

General procedure for the preparation of 2,6-diphenyl-pyrido[2,3-d]pyrimidin-7(8H)-ones (15–40). Exemplified for 6-(2,4-dichlorophenyl)-2-((4-(2-(diethylamino)ethoxy)phenyl) amino)-8-methylpyrido[2,3-d]pyrimidin-7(8H)-one (15). To a solution of **A13a** (30 mg, 0.13 mmol) in THF (0.5 mL) and DMF (0.5 mL) was added 60% NaH (8 mg, 0.33 mmol) at 0 °C. The mixture was stirred for 30 min at rt under argon. The mixture was cooled to 0 °C and then **A11a** (25 mg, 0.06 mmol) was added. The reaction mixture was stirred at rt for 2 h. The reaction mixture was quenched by addition of ice and NaOH (0.5 mL, 2N) solution and then partitioned between water and EtOAc. The organic layer was

dried over anhydrous Na_2SO_4, filtered and concentrated to give a residue that was purified by column chromatography using silica gel (5% MeOH/DCM) to afford **15** as a yellow solid (74% yield). ^{1}H NMR (600 MHz, $CDCl_3$) δ 8.54 (s, 1H), 7.55 (d, J = 7.8 Hz, 4H), 7.49 (s, 1H), 7.30 (s, 2H), 6.94 (d, J = 9.2 Hz, 2H), 4.07 (t, J = 6.2 Hz, 2H), 3.75 (s, 3H), 2.89 (t, J = 6.2 Hz, 2H), 2.65 (q, J = 7.2 Hz, 4H), 1.08 (t, J = 7.1 Hz, 6H). ^{13}C NMR (150 MHz, $CDCl_3$) δ 162.1, 159.4, 158.6, 155.9, 155.6, 135.7, 134.7, 134.6, 133.7, 132.6, 131.5, 129.7, 127.1, 126.5, 122.0, 115.0, 106.4, 66.9, 51.8, 47.9, 28.6, 11.9. HRMS *m/z* calculated for $C_{26}H_{27}Cl_2N_5O_2$ $[M + H]^+$: 512.1615; found 512.1626. Purity 95.6% (t_R 21.56 min), mp 245–247 °C.

6-(2-Chlorophenyl)-2-((4-(2-(diethylamino)ethoxy)phenyl) amino)-8-methylpyrido[2,3-d]pyrimidin-7(8H)-one (16). Synthesized from **A11b** and **A13a** by using the general procedure for **15** to give **16** (62%) as a yellow solid. ^{1}H NMR (400 MHz, $CDCl_3$) δ 8.54 (s, 1H), 7.55 (d, J = 6.9 Hz, 3H), 7.48–7.45 (m, 1H), 7.37–7.30 (m, 3H), 6.94 (d, J = 8.7 Hz, 2H), 4.07 (t, J = 6.4 Hz, 2H), 3.76 (s, 3H), 2.89 (t, J = 6.2 Hz, 2H), 2.65 (q, J = 7.2 Hz, 4H), 1.08 (t, J = 7.3 Hz, 6H). ^{13}C NMR (100 MHz, $CDCl_3$) δ 162.3, 159.3, 158.5, 155.9, 155.5, 135.5, 135.2, 133.9, 131.7, 131.6, 129.8, 129.5, 127.8, 126.7, 122.0, 115.0, 106.5, 66.9, 51.8, 47.9, 28.6, 11.9. HRMS *m/z* calculated for $C_{26}H_{28}ClN_5O_2$ $[M + H]^+$: 478.2004; found 478.2007. Purity 99.15% (t_R 19.93 min), mp 193–195 °C.

6-(4-Chlorophenyl)-2-((4-(2-(diethylamino)ethoxy)phenyl) amino)-8-methylpyrido[2,3-d]pyrimidin-7(8H)-one (17). Synthesized from **A11d** and **A13a** by using the general procedure for **15** to give **17** (45%) as a yellow solid. ^{1}H NMR (400 MHz, $CDCl_3$) δ 8.56 (s, 1H), 7.62–7.60 (m, 3H), 7.54 (d, J = 8.8 Hz, 2H), 7.38 (d, J = 8.8 Hz, 2H), 6.94 (d, J = 8.8 Hz, 2H), 4.07 (t, J = 6.2 Hz, 2H), 3.75 (s, 3H), 2.89 (t, J = 6.2 Hz, 2H), 2.66 (q, J = 7.2 Hz, 4H), 1.08 (t, J = 7.3 Hz, 6H). ^{13}C NMR (150 MHz, $CDCl_3$) δ 162.7, 159.1, 158.4, 155.4, 155.3, 134.6, 134.0, 133.3, 131.7, 130.1, 128.5, 127.8, 122.0, 115.0, 106.9, 66.6, 51.7, 47.8, 28.6, 11.6. HRMS *m/z* calculated for $C_{26}H_{28}ClN_5O_2$ $[M + H]^+$: 478.2004; found 478.2010. Purity 96.5% (t_R 21.33 min), mp 216–218 °C.

6-(4-(*Tert*-butyl)phenyl)-2-((4-(2-(diethylamino)ethoxy) phenyl)amino)-8-methylpyrido[2,3-d]pyrimidin-7(8H)-one (18). Synthesized from **A11e** and **A13a** by using the general procedure for **15** to give **18** (58%) as a yellow solid. ^{1}H NMR (400 MHz, $CDCl_3$) δ 8.54 (s, 1H), 7.63–7.59 (m, 3H), 7.56 (d, J = 8.8 Hz, 2H), 7.45 (d, J = 8.4 Hz, 2H), 6.94 (d, J = 8.8 Hz, 2H), 4.07 (t, J = 6.4 Hz, 2H), 3.76 (s, 3H), 2.89 (t, J = 6.4 Hz, 2H), 2.65 (q, J = 7.2 Hz, 4H), 1.35 (s, 9H), 1.08 (t, J = 7.1 Hz, 6H). ^{13}C NMR (100 MHz, $CDCl_3$) δ 163.1, 159.0, 158.1, 155.4, 155.3, 151.2, 133.3, 132.8, 131.8, 129.1, 128.5, 125.3, 121.9, 114.9, 107.2, 66.9, 51.8, 47.9, 34.7, 31.4, 28.6, 11.9. HRMS *m/z* calculated for $C_{30}H_{37}N_5O_2$ $[M + H]^+$: 500.3020; found 500.3028. Purity 99.8% (t_R 23.44 min), mp 208–210 °C.

2-((4-(2-(Diethylamino)ethoxy)phenyl)amino)-6-(4-hydroxyphenyl)-8-methylpyrido[2,3-d]pyrimidin-7(8H)-one (19). Synthesized from **A11k** and **A13a** by using the general procedure for **15** to give **19** (64%) as pale yellow solid. Note the TBS-protecting group from **A11k** was removed during the reaction. ^{1}H NMR (400 MHz, CD_3OD) δ 8.66 (s, 1H), 7.79 (s, 1H), 7.68 (d, J = 9.2 Hz, 2H), 7.50 (d, J = 8.8 Hz, 2H), 6.99 (d, J = 9.2 Hz, 2H), 6.83 (d, J = 8.8 Hz, 2H), 4.25 (t, J = 5.2 Hz, 2H), 3.74 (s, 3H), 3.36–3.34 (m, 2H), 3.11 (q, J = 7.2 Hz, 4H), 1.28 (t, J = 7.4 Hz, 6H). HRMS *m/z* calculated for $C_{26}H_{29}N_5O_3$ $[M + H]^+$: 460.2343; found 460.2348. Purity 99.82% (t_R 17.44 min), mp 215–217 °C.

2-((4-(2-(Diethylamino)ethoxy)phenyl)amino)-6-(4-methoxyphenyl)-8-methylpyrido[2,3-d]pyrimidin-7(8H)-one (20). Synthesized from **A11l** and **A13a** by using the general procedure for **15** to give **20** (66%) as yellow solid. ^{1}H NMR (400 MHz, CD_3OD) δ 8.59 (s, 1H), 7.73 (s, 1H), 7.61 (d, J = 8.4 Hz, 2H), 7.55 (d, J = 8.8 Hz, 2H), 6.94–6.90 (m, 4H), 4.11 (t, J = 5.4 Hz, 2H), 3.80 (s, 3H), 3.68 (s, 3H), 3.04 (t, J = 5.2 Hz, 2H), 2.82 (q, J = 7.2 Hz, 4H), 1.16 (t, J = 7 Hz, 6H). HRMS *m/z* calculated for $C_{27}H_{31}N_5O_3$ $[M + H]^+$: 474.2500; found 474.2505. Purity 98.89% (t_R 19.86 min), mp 188–190 °C.

2-((4-(2-(Diethylamino)ethoxy)phenyl)amino)-8-methyl-6-phenylpyrido[2,3-d]pyrimidin-7(8H)-one (21). Synthesized from **A11c** and **A13a** by using the general procedure for **15** to give **21** (64%) as a yellow solid. ^{1}H NMR (400 MHz, $CDCl_3$) δ 8.55 (s, 1H), 7.68–7.63 (m, 3H), 7.56 (d, J = 8.7 Hz, 2H), 7.45–7.33 (m, 3H), 6.94 (td, J = 6.2, 4.1 Hz, 2H), 4.12 (t, J = 6.2 Hz, 2H), 3.77 (s, 3H), 2.96 (t, J = 6.2 Hz, 2H), 2.73 (q, J = 7.2 Hz, 4H), 1.13 (t, J = 7.1 Hz, 6H). ^{13}C NMR (100 MHz, $CDCl_3$) δ 162.9, 159.0, 158.3, 155.4, 155.2, 136.2, 133.3, 131.9, 129.2, 128.9, 128.3, 128.2, 121.9, 115.0, 107.1, 66.4, 51.7, 47.8, 28.6, 11.5. HRMS *m/z* calculated for $C_{26}H_{29}N_5O_2$ $[M + H]^+$: 444.2394; found 444.2397. Purity 99.4% (t_R 19.75 min), mp 172–174 °C.

2-((4-(2-(Diethylamino)ethoxy)phenyl)amino)-8-ethyl-6-phenylpyrido[2,3-d]pyrimidin-7(8H)-one (22). Synthesized from **A11m** and **A13a** by using the general procedure for **15** to give **22** (54%) as a yellow solid. ^{1}H NMR (400 MHz, $CDCl_3$) δ 8.56 (s, 1H), 7.67 (d, J = 3.6 Hz, 2H), 7.64 (s, 1H), 7.56 (d, J = 9.2 Hz, 2H), 7.46–7.30 (m, 3H), 6.94 (d, J = 8.8 Hz, 2H), 4.50 (q, J = 7.0 Hz, 2H), 4.07 (t, J = 6.2 Hz, 2H), 2.90 (t, J = 6.2 Hz, 2H), 2.66 (q, J = 7.0 Hz, 4H), 1.38 (t, J = 7.1 Hz, 3H), 1.09 (t, J = 7.1 Hz, 6H). HRMS *m/z* calculated for $C_{27}H_{31}N_5O_2$ $[M + H]^+$: 458.2551; found 458.2556. Purity 95.8% (t_R 20.50 min), mp 133–135 °C.

2-((4-(2-(Diethylamino)ethoxy)phenyl)amino)-8-(2-hydroxyethyl)-6-phenylpyrido[2,3-d]pyrimidin-7(8H)-one (23). Synthesized from **A11n** and **A13a** by using the general procedure for **15** to give **23** (33%) as a yellow solid. ^{1}H NMR (600 MHz, CD_3OD) δ 8.70 (s, 1H), 7.88 (s, 1H), 7.68 (d, J = 7.8 Hz, 2H), 7.64 (d, J = 7.8 Hz, 2H), 7.41 (t, J = 7.5 Hz, 2H), 7.35 (d, J = 7.5 Hz, 1H), 7.01 (d, J = 9Hz, 2H), 4.63 (t, J = 6.3 Hz, 2H), 4.27 (t, J = 4.8 Hz, 2H), 3.89 (t, J = 6.6 Hz, 2H), 3.37–3.34 (m, 2H), 3.13–3.12 (m, 4H), 1.28 (t, J = 7.2 Hz, 6H). HRMS *m/z* calculated for $C_{27}H_{31}N_5O_3$ $[M + H]^+$: 474.2500; found 474.2504. Purity 95.0% (t_R 18.48 min), mp 157–159 °C.

6-(2,6-Dichlorophenyl)-2-((4-(2-(diethylamino)ethoxy) phenyl)amino)-8-(2-methoxyethyl)pyrido[2,3-d]pyrimidin-7(8H)-one (24). Synthesized from **A11o** and **A13a** by using the general procedure for **15** to give **24** (61%) as a yellow solid. ^{1}H NMR (400 MHz, $CDCl_3$) δ 8.55 (s, 1H), 7.56–7.51 (m, 3H), 7.41 (d, J = 8 Hz, 3H), 7.28–7.24 (m, 1H), 6.94 (d, J = 9.2 Hz, 2H), 4.66 (t, J = 6 Hz, 2H), 4.06 (t, J = 6.4 Hz, 2H), 3.76 (t, J = 6.2 Hz, 2H), 3.36 (s, 3H), 2.89 (t, J = 6.2 Hz, 2H), 2.66 (q, J = 7.2 Hz, 4H), 1.08 (t, J = 7.2 Hz, 6H). ^{13}C NMR (100 MHz, $CDCl_3$) δ 161.2, 159.5, 158.8, 155.9, 155.6, 136.6, 135.8, 134.2, 131.5, 129.9, 128.1, 125.7, 122.2, 114.9, 106.4, 69.1, 66.9, 58.9, 51.8, 47.9, 40.4, 11.9. HRMS *m/z* calculated for $C_{28}H_{31}Cl_2N_5O_3$ $[M + H]^+$: 556.1877; found 556.1879. Purity 97.4% (t_R 20.76 min), mp 133–135 °C.

8-Benzyl-6-(2,6-dichlorophenyl)-2-((4-(2-(diethylamino) ethoxy)phenyl)amino)pyrido[2,3-d]pyrimidin-7(8H)-one (25). Synthesized from **A11p** and **A13a** by using the general procedure for **15** to give **25** (68%) as a yellow solid. ^{1}H NMR (400 MHz, $CDCl_3$) δ 8.54 (s, 1H), 7.53 (s, 1H), 7.41–7.19 (m, 11H), 6.91 (d, J = 9.2 Hz, 2H), 5.60 (s, 2H), 4.08 (t, J = 6.4 Hz, 2H), 2.90 (t, J = 6.2 Hz, 2H), 2.67 (q, J = 7.2 Hz, 4H), 1.09 (t, J = 7.3 Hz, 6H). ^{13}C NMR (100 MHz, $CDCl_3$) δ 161.4, 159.7, 158.8, 155.9, 155.7, 137.0, 136.7, 135.8, 134.3, 131.3, 129.9, 128.4, 128.2, 128.1, 127.3, 125.9, 123.1, 114.9, 106.4, 66.8, 51.8, 47.9, 44.5, 11.9. HRMS *m/z* calculated for $C_{32}H_{31}Cl_2N_5O_2$ $[M + H]^+$: 588.1928; found 588.1932. Purity 98.4% (t_R 22.59 min), mp 163–165 °C.

6-(2,6-Dichlorophenyl)-2-((4-(2-(diethylamino)ethoxy) phenyl)amino)-8-isobutylpyrido[2,3-d]pyrimidin-7(8H)-one (26). Synthesized from **A11q** and **A13a** by using the general procedure for **15** to give **26** (36%) as a yellow solid. ^{1}H NMR (400 MHz, $CDCl_3$) δ 8.54 (s, 1H), 7.83 (brs, 1H), 7.57 (d, J = 9.2 Hz, 2H), 7.49 (s,

1H), 7.38 (d, J = 7.8 Hz, 2H), 7.23 (d, J = 8.2 Hz, 1H), 6.93 (d, J = 9.2 Hz, 2H), 4.28 (d, J = 7.3 Hz, 2H), 4.07 (t, J = 6.2 Hz, 2H), 2.90 (t, J = 6.2 Hz, 2H), 2.66 (q, J = 7.0 Hz, 4H), 2.42–2.31 (sep, J = 6.8, 7.2 Hz, 1H), 1.09 (t, J = 7.1 Hz, 6H), 0.97 (d, J = 6.4 Hz, 6H). ^{13}C NMR (100 MHz, $CDCl_3$) δ 161.6, 159.3, 158.6, 155.9, 155.4, 136.3, 135.8, 134.4, 131.8, 129.8, 128.1, 125.9, 122.0, 114.8, 106.3, 66.8, 51.8, 48.3, 47.9, 27.4, 20.3, 11.8. HRMS *m/z* calculated for $C_{29}H_{33}Cl_2N_5O_2$ [M + H]$^+$: 554.2084; found 554.2085. Purity 97.7% (t_R 22.55 min), mp 196–198 °C.

6-(2,6-Dichlorophenyl)-2-((4-(2-(diethylamino)ethoxy) phenyl)amino)-8-(3-(methylsulfonyl)benzyl)pyrido[2,3-d]pyrimidin-7(8H)-one (27). Synthesized from **A11s** and **A13a** by using the general procedure for **15** to give **27** (84%) as pale yellow solid. ^{1}H NMR (600 MHz, $CDCl_3$) δ 8.58 (s, 1H), 7.99 (s, 1H), 7.81 (d, J = 7.8 Hz, 1H), 7.60–7.39 (m, 7H), 7.32–7.26 (m, 2H), 6.94 (d, J = 9 Hz, 2H), 5.68 (s, 2H), 4.10 (t, J = 5.7 Hz, 2H), 2.93–2.91 (m, 5H), 2.68 (q, J = 7.2 Hz, 4H), 1.09 (t, J = 7.2 Hz, 6H). HRMS *m/z* calculated for $C_{33}H_{33}Cl_2N_5O_4S$ [M + H]$^+$: 666.1703; found 666.1703. Purity 95.67% (t_R 21.35 min), mp 203–205 °C.

6-(2,6-Dichlorophenyl)-2-((4-(2-(diethylamino)ethoxy) phenyl)amino)-8-(4-(methylsulfonyl)benzyl)pyrido[2,3-d]pyrimidin-7(8H)-one (28). Synthesized from **A11t** and **A13a** by using the general procedure for **15** to give **28** (70%) as pale yellow solid. ^{1}H NMR (600 MHz, $CDCl_3$) δ 8.58 (s, 1H), 7.81 (d, J = 8.4 Hz, 2H), 7.57 (s, 1H), 7.49–7.36 (m, 6H), 7.29–7.26 (m, 2H), 6.92 (d, J = 8.4 Hz, 2H), 5.64 (s, 2H), 4.08 (t, J = 6.3 Hz, 2H), 3.00 (s, 3H), 2.91 (t, J = 6 Hz, 2H), 2.67 (t, J = 7.2 Hz, 4H), 1.09 (t, J = 6.9 Hz, 6H). HRMS *m/z* calculated for $C_{33}H_{33}Cl_2N_5O_4S$ [M + H]$^+$: 666.1703; found 666.1716. Purity 95.61% (t_R 21.24 min), mp 208–210 °C.

6-(2,6-Dichlorophenyl)-8-methyl-2-((4-(methylsulfonyl) phenyl)amino)pyrido[2,3-d]pyrimidin-7(8H)-one (29). Synthesized from **A11f** and **A13b** by using the general procedure for **15** to give **29** (75%) as a white solid. ^{1}H NMR (400 MHz, $CDCl_3$) δ 8.67 (s, 1H), 7.99–7.91 (m, 4H), 7.78 (s, 1H), 7.79 (s, 1H), 7.42 (d, J = 7.8 Hz, 2H), 7.32–7.28 (m, 1H), 3.83 (s, 3H), 3.09 (s, 3H). ^{13}C NMR (100 MHz, $CDCl_3$) δ 161.3, 158.5, 158.4, 155.9, 143.8, 136.1, 135.6, 134.0, 133.9, 130.2, 129.0, 128.2, 127.5, 119.0, 107.7, 44.9, 28.9. HRMS *m/z* calculated for $C_{21}H_{16}Cl_2N_4O_3S$ [M + H]$^+$: 475.0393; found 475.0397. Purity 97.6% (t_R 22.92 min), mp 298–300 °C.

6-(2,6-Dichlorophenyl)-8-methyl-2-((3-(methylsulfonyl) phenyl)amino)pyrido[2,3-d]pyrimidin-7(8H)-one (30). Synthesized from **A11f** and **A13c** by using the general procedure for **15** to give **30** (92%) as a white solid. ^{1}H NMR (400 MHz, $CDCl_3$) δ 8.69 (d, J = 14.2 Hz, 2H), 8.22 (s, 1H), 7.82 (d, J = 8 Hz, 1H), 7.65 (d, J = 7.2 Hz, 1H), 7.59 (t, J = 4.2 Hz, 2H), 7.41 (d, J = 8 Hz, 2H), 7.31–7.25 (m, 1H), 3.86 (s, 3H), 3.11 (s, 3H). ^{13}C NMR (100 MHz, $CDCl_3$) δ 161.4, 158.7, 158.6, 155.9, 141.4, 140.0, 136.2, 135.7, 134.0, 130.2, 130.1, 128.1, 127.1, 124.1, 121.6, 118.0, 107.3, 44.6, 29.0. HRMS *m/z* calculated for $C_{21}H_{16}Cl_2N_4O_3S$ [M + H]$^+$: 475.0393; found 475.0393. Purity 98.2% (t_R 22.98 min), mp 238–240 °C.

6-(4-Chlorophenyl)-8-methyl-2-((3-(methylsulfonyl)phenyl) amino)pyrido[2,3-d]pyrimidin-7(8H)-one (31). Synthesized from **A11d** and **A13c** by using the general procedure for **15** to give **31** (61%) as a pale yellow solid. ^{1}H NMR (400 MHz, DMSO-d_6) δ 10.59 (s, 1H), 8.90 (s, 1H), 8.78 (s, 1H), 8.11 (s, 1H), 7.95 (d, J = 8 Hz, 1H), 7.73 (d, J = 8.8 Hz, 2H), 7.63 (t, J = 7.8 Hz, 1H), 7.58 (d, J = 8.4 Hz, 1H), 7.51 (d, J = 8.8 Hz, 2H), 3.71(s, 3H), 3.22 (s, 3H). HRMS *m/z* calculated for $C_{21}H_{17}ClN_4O_3S$ [M + H]$^+$: 441.0783; found 441.0781. Purity 98.15% (t_R 23.99 min), mp 296–298 °C.

6-(4-Chlorophenyl)-8-isobutyl-2-((3-(methylsulfonyl) phenyl)amino)pyrido[2,3-d]pyrimidin-7(8H)-one (32). Synthesized from **A11r** and **A13c** by using the general procedure for **15** to give **32** (33%) as a pale yellow solid. ^{1}H NMR (400 MHz, $CDCl_3$) δ 8.66 (s, 1H), 8.32 (t, J = 1.8 Hz, 1H), 8.05 (d, J = 8.2 Hz, 1H), 7.74 (s, 1H), 7.71–7.56 (m, 5H), 7.41 (d, J = 8.8 Hz, 2H), 4.38 (d, J = 7.2 Hz, 2H), 3.11 (s, 3H), 2.40–2.30 (sep, J = 6.8, 8.4 Hz, 1H), 0.99 (d, J = 6.4 Hz, 6H). HRMS *m/z* calculated for $C_{24}H_{23}ClN_4O_3S$ [M + H]$^+$: 483.1252; found 483.1261. Purity 97.49% (t_R 26.82 min), mp 225–227 °C.

6-(2-Chlorophenyl)-8-methyl-2-((3-(methylsulfonyl)phenyl) amino)pyrido[2,3-d]pyrimidin-7(8H)-one (33). Synthesized from **A11b** and **A13c** by using the general procedure for **15** to give **33** (72%) as a white solid. ^{1}H NMR (500 MHz, $CDCl_3$) δ 8.70 (s, 1H), 8.64 (s, 1H), 7.84 (brs, 1H), 7.79 (d, J = 7.2 Hz, 1H), 7.66 (d, J = 9 Hz, 1H), 7.63 (s, 1H), 7.58 (t, J = 7.8 Hz, 1H), 7.49–7.47 (m, 1H), 7.38–7.32 (m, 3H), 3.85 (s, 3H), 3.10 (s, 3H). ^{13}C NMR (150 MHz, $CDCl_3$) δ 162.1, 158.5, 158.4, 155.7, 141.5, 140.0, 135.1, 134.9, 133.8, 131.6, 130.2, 129.8, 129.7, 129.3, 126.8, 123.9, 121.5, 117.9, 107.5, 44.6, 28.9. HRMS *m/z* calculated for $C_{21}H_{17}ClN_4O_3S$ [M + H]$^+$: 441.0783; found 441.0784. Purity 98.1% (t_R 22.36 min), mp 230–232 °C.

6-(2,4-Dichlorophenyl)-8-methyl-2-((3-(methylsulfonyl) phenyl)amino)pyrido[2,3-d]pyrimidin-7(8H)-one (34). Synthesized from **A11a** and **A13c** by using the general procedure for **15** to give **34** (63%) as a pale yellow solid. ^{1}H NMR (500 MHz, $CDCl_3$) δ 8.70 (s, 1H), 8.65 (s, 1H), 7.78 (d, J = 6.5 Hz, 2H), 7.67–7.56 (m, 3H), 7.50 (s, 1H), 7.32 (s, 2H), 3.84 (s, 3H), 3.10 (s, 3H). ^{13}C NMR (125 MHz, $CDCl_3$) δ 162.0, 158.6, 158.5, 155.7, 141.5, 139.9, 135.4, 134.9, 134.6, 133.4, 132.5, 130.2, 129.7, 128.0, 127.2, 123.9, 121.6, 118.0, 107.4, 44.6, 29.0. HRMS *m/z* calculated for $C_{21}H_{16}Cl_2N_4O_3S$ [M + H]$^+$: 475.0393; found 475.0400. Purity 99.5% (t_R 24.04 min), mp 231–233 °C.

6-(2,3-Dichlorophenyl)-8-methyl-2-((3-(methylsulfonyl) phenyl)amino)pyrido[2,3-d]pyrimidin-7(8H)-one (35). Synthesized from **A11g** and **A13c** by using the general procedure for **15** to give **35** (68%) as a pale yellow solid. ^{1}H NMR (600 MHz, DMSO-d_6) δ 10.64 (s, 1H), 8.90 (s, 1H), 8.77 (s, 1H), 7.96 (m, 2H), 7.70 (d, J = 7.8 Hz, 1H), 7.63 (t, J = 8.1 Hz, 1H), 7.58 (d, J = 8.4 Hz, 1H), 7.45 (t, J = 7.8 Hz, 1H), 7.39 (d, J = 7.8 Hz, 1H), 3.69 (s, 3H), 3.23 (s, 3H). ^{13}C NMR (150 MHz, DMSO-d_6) δ 161.4, 159.9, 159.2, 155.6, 141.9, 141.0, 138.5, 136.3, 132.3, 131.9, 131.0, 130.7, 130.4, 128.7, 127.6, 124.4, 120.9, 117.6, 106.9, 44.2, 28.7. HRMS *m/z* calculated for $C_{21}H_{16}Cl_2N_4O_3S$ [M + H]$^+$: 475.0393; found 475.0397. Purity 98.5% (t_R 23.50 min), mp 270–272 °C.

6-(2-Chloro-4-fluorophenyl)-8-methyl-2-((3-(methylsulfonyl)phenyl)amino)pyrido[2,3-d]pyrimidin-7(8H)-one (36). Synthesized from **A11h** and **A13c** by using the general procedure for **15** to give **36** (60%) as a white solid. ^{1}H NMR (600 MHz, DMSO-d_6) δ 10.63 (s, 1H), 8.90 (s, 1H), 8.77 (brs, 1H), 7.96 (d, J = 7.8 Hz, 1H), 7.93 (s, 1H), 7.63 (t, J = 8.1 Hz, 1H), 7.59–7.56 (m, 2H), 7.49–7.46 (m, 1H), 7.36 (td, J = 8.5, 3 Hz, 1H), 3.69 (s, 3H), 3.22 (s, 3H). ^{13}C NMR (150 MHz, DMSO-d_6) δ 162.9, 161.7, 161.3, 159.8, 159.1, 155.5, 141.9, 141.0, 136.6, 134.6, 134.5, 133.9, 132.5, 130.4, 126.8, 124.4, 120.9, 117.6, 117.2, 117.0, 114.9, 114.7, 106.9, 44.2, 28.7. HRMS *m/z* calculated for $C_{21}H_{16}ClFN_4O_3S$ [M + H]$^+$: 459.0688; found 459.0688. Purity 97.6% (t_R 22.72 min), mp 248–250 °C.

6-(2,5-Dichlorophenyl)-8-methyl-2-((3-(methylsulfonyl) phenyl)amino)pyrido[2,3-d]pyrimidin-7(8H)-one (37). Synthesized from **A11i** and **A13c** by using the general procedure for **15** to give **37** (92%) as a white solid. ^{1}H NMR (400 MHz, DMSO-d_6) δ 10.66 (s, 1H), 8.90 (s, 1H), 8.77 (s, 1H), 7.99–7.96 (m, 2H), 7.66–7.57 (m, 3H), 7.54–7.51 (m, 2H), 3.69 (s, 3H), 3.23 (s, 3H). HRMS *m/z* calculated for $C_{21}H_{16}Cl_2N_4O_3S$ [M + H]$^+$: 475.0393; found 475.0390. Purity 97.4% (t_R 23.76 min), mp 263–265 °C.

Preparation of 6-chloro-8-methyl-2-(methylthio)pyrido[2,3-d]pyrimidin-7(8H)-one (A14). The mixture of **A7** (20 mg, 0.11 mmol) and 60% NaH (8 mg, 0.33 mmol) in THF (1.5 mL) was stirred at rt for 10 min under argon. A solution of ethyl 2-chloro-2-(diethoxyphosphoryl)acetate (42 mg, 0.16 mmol) in THF (0.5 mL) was added dropwise to and the resulting mixture was heated at reflux for 2.5 h. The reaction mixture was cooled to rt, concentrated and extracted using EtOAc and water. The organic layer was dried

over anhydrous Na_2SO_4, filtered and concentrated to give a residue that was purified by column chromatography using silica gel (30% EtOAc/Hexane) to afford **A14** as a white solid (42% yield). ^{1}H NMR (600 MHz, $CDCl_3$) δ 8.59 (s, 1H), 7.82 (s, 1H), 3.80 (s, 3H), 2.62 (s, 3H). ^{13}C NMR (150 MHz, $CDCl_3$) δ (ppm) 173.6, 159.3, 155.7, 153.3, 132.6, 126.7, 109.0, 29.2, 14.6.

6-(2-Chloro-4-methylphenyl)-8-methyl-2-(methylthio)pyrido[2,3-d]pyrimidin-7(8H)-one (A15). A14 (24 mg, 0.11 mmol), (2-chloro-4-methylphenyl)boronic acid (28 mg, 0.16 mmol) and $Pd(PPh_3)_4$ (13 mg, 0.011 mmol) were placed in a round-bottom flask and purged with argon for 10 min. DMF (1 mL) and CH_3CN (2 mL) were added and the flask was again purged with argon for 10 min. A 1M solution of Na_2CO_3 (23 mg, 0.21 mmol) (220 μL) was added dropwise and the reaction mixture was heated at 90 °C for 5 h. The reaction mixture was allowed to cool to rt, the solvent was evaporated, and the residue was partitioned between water and EtOAc. The organic layer was dried over anhydrous Na_2SO_4, filtered and concentrated to give a residue that was purified by column chromatography using silica gel (10% EtOAc/DCM) to afford **A15** as a white solid (57%). ^{1}H NMR (400 MHz, $CDCl_3$) δ 8.64 (s, 1H), 7.64 (s, 1H), 7.31–7.23 (m, 2H), 7.14 (d, J = 7.6 Hz, 1H), 3.82 (s, 3H), 2.66 (s, 3H), 2.38 (s, 3H). ^{13}C NMR (100 MHz, $CDCl_3$) δ 173.3, 161.9, 156.3, 154.3, 140.3, 134.8, 133.3, 131.6, 131.2, 130.4, 127.7, 109.4, 28.5, 21.1, 14.6.

6-(2-Chloro-4-methylphenyl)-8-methyl-2-(methylsulfonyl) pyrido[2,3-d]pyrimidin-7(8H)-one (A16). This compound was synthesized by using the general procedure for the preparation of **A11a**. White solid (68% yield): ^{1}H NMR (400 MHz, $CDCl_3$) δ 8.99 (s, 1H), 7.80 (s, 1H), 7.34 (s, 1H), 7.27–7.24 (m, 1H), 7.17 (d, J = 8.4 Hz, 1H), 3.89 (s, 3H), 3.44 (s, 3H), 2.41 (s, 3H). ^{13}C NMR (100 MHz, $CDCl_3$) δ 164.4, 161.3, 157.1, 155.1, 141.2, 136.6, 133.6, 133.1, 130.9, 130.6, 130.5, 127.8, 115.1, 39.3, 29.3, 21.2.

6-(2-Chloro-4-methylphenyl)-8-methyl-2-((3-(methylsulfonyl)phenyl)amino)pyrido[2,3-d]pyrimidin-7(8H)-one (38). Synthesized from **A16** and **A13c** by using the general procedure for **15** to give **38** (75%) as a white solid. ^{1}H NMR (400 MHz, DMSO-d_6) δ 10.61 (s, 1H), 8.89 (s, 1H), 8.77 (s, 1H), 7.97 (d, J = 8.8 Hz, 1H), 7.88 (s, 1H), 7.65–7.57 (m, 2H), 7.39 (s, 1H), 7.29 (d, J = 8 Hz, 1H), 7.22 (d, J = 7.7 Hz, 1H), 3.69 (s, 3H), 3.23 (s, 3H), 2.36 (s, 3H). HRMS *m/z* calculated for $C_{22}H_{19}ClN_4O_3S$ $[M + H]^+$: 455.0939; found 455.0944. Purity 99.6% (t_R 23.51 min), mp 182–184 °C.

6-(4-Hydroxyphenyl)-8-methyl-2-((3-(methylsulfonyl) phenyl)amino)pyrido[2,3-d]pyrimidin-7(8H)-one (39). Synthesized from **A11k** and **A13c** by using the general procedure for **15** to give **39** (79%) as pale yellow solid. Note the TBS-protecting group from **A11k** was removed during the reaction. ^{1}H NMR (400 MHz, DMSO-d_6) δ 10.53 (s, 1H), 9.63 (s, 1H), 8.87 (s, 1H), 8.79 (s, 1H), 7.95–7.94 (m, 2H), 7.62 (t, J = 7.8 Hz, 1H), 7.57–7.53 (m, 3H), 6.82 (d, J = 8.8 Hz, 2H), 3.70 (s, 3H), 3.22 (s, 3H). HRMS *m/z* calculated for $C_{21}H_{18}N_4O_4S$ $[M + H]^+$: 423.1122; found 423.1120. Purity 95.0% (t_R 19.63 min), mp 268–270 °C.

6-(4-Methoxyphenyl)-8-methyl-2-((3-(methylsulfonyl) phenyl)amino)pyrido[2,3-d]pyrimidin-7(8H)-one (40). Synthesized from **A11l** and **A13c** by using the general procedure for **15** to give **40** (95%) as yellow solid. ^{1}H NMR (400 MHz, DMSO-d_6) δ 10.52 (s, 1H), 8.87–8.77 (m, 2H), 7.99–7.94 (m, 2H), 7.66–7.54 (m, 4H), 6.99 (d, J = 8.4 Hz, 2H), 3.79 (s, 3H), 3.70 (s, 3H), 3.21 (s, 3H). HRMS *m/z* calculated for $C_{22}H_{20}N_4O_4S$ $[M + H]^+$: 437.1278; found 437.1282. Purity 97.52% (t_R 22.42 min), mp 291–293 °C.

Molecular docking studies. AutoDock 4.2 (AutoDock Tools 1.5.6) was used to perform molecular docking studies. Ligands were docked into the ATP binding site of the protein using the ligand docking protocol in AutoDock 4.2. The structure of the protein was kept rigid, while the ligand structures were set partially flexible by setting the number of rotatable bonds. In brief, ligands were built using ChemBio3D and subjected to MM2 (force field) energy minimization. Using AutoGrid, the grid box was set to 70.00 Å, 60 Å and 50 Å along the x-, y- and z-axis, with 0.375 Å spacing. Docking calculations were carried out using the Lamarckian genetic algorithm with default parameters. Docking poses were selected based on the hydrogen bond interaction between the pyrimidine nitrogen (N-3) and amino –NH of the pyrido[2,3-d]pyrimidin-7-one with RIPK2 hinge residue Met98 and the highest binding energy (kcal/mol). Docking pose analyses were performed using the PyMOL Molecular Graphics System, Version 2.0 Schrodinger LLC software.

ADPGlo kinase assay. Recombinant RIPK2 protein (20 ng per reaction) was diluted in the reaction buffer consisting of 40 mM Tris (pH 7.5); 20 mM $MgCl_2$; 0.1 mg/ml BSA; 50 μM DTT. Diluted protein was added to low volume white 384 well plates (2 μL/well). Inhibitors were diluted 1:3 in reaction buffer, and then 1 μL was added to each well and incubated 5 min at room temperature. Reactions were initiated by the addition of 2 μL of 100 μM ATP and 1 mg/ml RS repeat peptide (SignalChem) in the reaction buffer. The final RIPK2 and substrate concentrations were 105 nM and 207 μM, respectively. Plates were sealed with plastic coverslips and incubated at room temperature for 2 h. Reactions were stopped by the addition of 5 μL of ADP-Glo reagent (Promega) and the ADP generation reaction was performed for 40 min at room temperature. Luminescence signal was generated by the addition of 10 μL of Kinase detection reagent (Promega) for 30 min at room temperature. Luminescence signals were determined using appropriate luminescence plate-reader (typical integration time 0.3–1 s). To calculate percent inhibition, the average background signal was subtracted from test well and maximal signal wells. Inhibition, % = (1- (test signal/maximal signal))*100. The percent inhibition at a specified concentration was determined or IC_{50} values were calculated based on a dose range of inhibitor concentrations using non-linear regression in GraphPad Prism software. Compound **12** [18] and DMSO were used as a positive and negative controls, respectively.

Radioisotope filter binding kinase assay. Enzyme inhibitory activity was evaluated by Reaction Biology Corp using a radiometric HotSpot™ assay system [34] by incubating human ALK2 with the protein substrate casein (1 mg/mL) and [ϒ-^{33}P] ATP (10 μM) in the presence of various concentrations of test compounds (10 nM–100 μM). After 30 min the amount of ^{33}P-casein was determined. A plot of inhibitor concentration versus % activity was constructed and from this plot, an IC_{50} value was determined.

NOD2-RIPK2 cellsignaling assay. HEK-Blue cells expressing human NOD2 and NFkB-SEAP reporter (Invivogen) were seeded into 96 well clear plates at 7.5x10^3 cells per well in 100 μL of DMEM media supplemented with 10% FBS and 1% antibiotic-antimycotic mix. Cells were allowed to attach for 48 h in 5% CO_2 tissue culture incubator at 37 °C. On the morning of the experiment, media in the wells was replaced with 100 μL of HEK-Blue detection media (Invivogen). Cells were treated with the inhibitors, diluted in DMSO (0.5 μL per well) for 15 min in 5% CO_2 tissue culture incubator at 37 °C. After that, cells were stimulated by the addition of 1 ng/well L18-MDP (Invivogen). Cells were incubated in 5% CO_2 tissue culture incubator at 37 °C for 8 h and absorbance, corresponding to the SEAP in the media, was determined in Wallac3V plate reader (Perkin Elmer). Inhibition, %= (1-((sample signal-unstimulated and DMSO treated cells)/(L18-MDP stimulated and DMSO treated cells - unstimulated and DMSO treated cells)))*100. IC_{50} values were calculated based on a dose range of inhibitor concentrations using non-linear regression in GraphPad Prism software.

Intracellular flow cytometry of CXCL8. U2OS/NOD2 cells including RIPK2 KO cells reconstituted with WT RIPK2 or T95W mutant are described in Hrdinka et al. [19]. Cells were treated with inhibitors and stimulated with L18-MDP (InvivoGen) as indicated in

figure legends. The intracellular staining of CXCL8 was performed as previously described [35]. The results were analyzed by FACS Canto Flow Cytometer (BD Biosciences, Franklin Lakes, NJ) and data processed using FlowJo software (FlowJo, LLC, Ashland, OR).

***In vitro* ADME studies of 33**. *In vitro* pharmacokinetic parameters such as metabolic stability ($t_{1/2}$ in hepatic microsomes and intrinsic clearance), solubility and permeability were performed for **33**. Hepatic microsomal stability was determined by incubating 1 μM compound with 1 mg/mL mouse hepatic microsomes in 100 mM potassium phosphate buffer, pH 7.4 at 37 °C with continuous shaking. NADPH was added with 1 mM final concentration to initiate the reaction and 40 μL aliquots were removed from 300 μL of the final incubation volume at different time points (0, 5, 10, 20, 40 and 60 min). These aliquots were then added to 160 μL acetonitrile to stop the reaction. NADPH dependence of the reaction was evaluated in parallel incubations without NADPH. The samples were centrifuged through a 0.45-μm filter plate at the end of the assay and analyzed by LC-MS/MS to determine the half-life of the compound. The kinetic aqueous solubility of **33** was determined by diluting 1 μL of a 10 mM DMSO stock with 99 μL PBS solution (pH 7.4), stored at room temperature for 24 h, filtered and analyzed by LC-MS/MS. These studies were performed by Cameron et al. at the Scripps Research Institute, Florida.

Pharmacokinetic study of 33. The pharmacokinetic study (Medicilon Preclinical Research LLC, Shanghai, China) was conducted in female ICR mice (N = 18) following a 10 mg/kg single intraperitoneal administration [formulated with DMSO (5%), solutol (10%) and water (85%)]. Blood samples were collected at 0.25, 0.5, 1, 2, 6, and 24 h. Brain samples were collected after 0.5 and 2 h. The plasma and brain concentrations of **33** were determined by liquid chromatography–tandem mass spectrometry. The lower limit of detection in plasma samples was 5 ng/mL, while in brain samples were 50 ng/mL.

Accession codes

PDB 5AR2 and 5J7B are available from the RCSB Protein Data Bank (https://www.rcsb.org/).

Declaration of competing interest

The authors declare the following financial interests/personal relationships which may be considered as potential competing interests: S.N., A.D. and G.D.C. declare the following financial interests/ personal relationships which may be considered as potential competing interests: PCT patent application (Publication Number: US 2020/0172536 A1) assigned to the University of Houston System and Trustees of Tufts College. All other authors declare no conflict of interest about this article. All other authors declare that they have no known competing financial interests or personal relationships that could have appeared to influence the work reported in this paper.

Acknowledgments

This work was supported in whole or in part with funds from the National Institutes of Health, Department of Health and Human Services (CA190542, AI124049, AG058642, AI144400 and NS111395). Work in the M.G-H laboratory was supported by the Ludwig Institute for Cancer Research Ltd. and a Wellcome Trust Senior Research Fellowship (102894/Z/13/Z).

Appendix A. Supplementary data

Supplementary data to this article can be found online at https://doi.org/10.1016/j.ejmech.2021.113252.

Abbreviations used

ADME	adsorption, distribution, metabolism and excretion
ALK2	activin receptor-like kinase 2
ADP	adenosine diphosphate
ATP	adenosine triphosphate
AUC	area under the curve
BRET	bioluminescence resonance energy transfer
BSA	bovine serum albumin
CARD	caspase-activated recruitment domain
CL	clearance
C_{max}	concentration maximum
CXCL8	C-X-C motif chemokine ligand 8
DAP	diaminopimelic acid
DFG	aspartic acid-phenyl alanine-glycine
DMEM	Dulbecco's modified eagle medium
DTT	dithiothreitol
FBS	fetal bovine serum
HEPES	(4-(2-hydroxyethyl)-1-piperazineethanesulfonic acid)
HPLC	high-performance liquid chromatography
HRMS	high resolution mass spectra
IC_{50}	half maximal inhibitory concentration
IKK	IκB kinase
IL	interleukin
ip	intraperitoneal
L18-MDP	lipidated form of muramyl dipeptide
LUBAC	linear ubiquitin chain assembly complex
MAPK	mitogen-activated protein kinase
NF-κB	nuclear factor kappa-light-chain-enhancer of activated B cells
NLR	NOD-like receptor
NOD	nucleotide-binding oligomerization domain
PAMPA	parallel artificial membrane permeability assay
PBS	phosphate-buffered saline
PDB	protein data bank
PG	peptidoglycan
PPI	protein-protein interaction
RIPK2	receptor-interacting protein kinase 2
SAR	structure-activity relationship
SEAP	secreted embryonic alkaline phosphatase
TAK1	transforming growth factor beta-activated kinase 1
TNF	tumor necrosis factor
Tris	tris(hydroxymethyl)aminomethane
Ub	ubiquitin
XIAP	X-linked inhibitor of apoptosis

References

[1] J.V. McCarthy, J. Ni, V.M. Dixit, RIP2 is a novel NF-κB-activating and cell death-inducing kinase, J. Biol. Chem. 273 (1998) 16968–16975, https://doi.org/10.1074/jbc.273.27.16968.

[2] M. Dorsch, A. Wang, H. Cheng, C. Lu, A. Bielecki, K. Charron, K. Clauser, H. Ren, R.D. Polakiewicz, T. Parsons, P. Li, T. Ocain, Y. Xu, Identification of a regulatory autophosphorylation site in the serine-threonine kinase RIP2, Cell. Signal. 18 (12) (2006) 2223–2229, https://doi.org/10.1016/j.cellsig.2006.05.005.

[3] S.E. Girardin, I.G. Boneca, J. Viala, M. Chamaillard, A. Labigne, G. Thomas, D.J. Philpott, P.J. Sansonetti, NOD2 is a general sensor of peptidoglycan through muramyl dipeptide (MDP) detection, J. Biol. Chem. 278 (2003) 8869–8872, https://doi.org/10.1074/jbc.c200651200.

[4] V. Fridh, K. Rittinger, The tandem CARDs of NOD2: intramolecular interactions and recognition of RIP2, PloS One 7 (3) (2012), e34375, https://doi.org/10.1371/journal.pone.0034375.

[5] R.B. Damgaard, U. Nachbur, M. Yabal, W.W. Wong, B.K. Fiil, M. Kastirr, E. Rieser, J.A. Rickard, A. Bankovacki, C. Peschel, J. Ruland, S. Bekker-Jensen, N. Mailand, T. Kaufmann, A. Strasser, H. Walczak, J. Silke, P.J. Jost, M. Gyrd-Hansen, The ubiquitin ligase XIAP recruits LUBAC for NOD2 signaling in inflammation and innate immunity, Mol. Cell 46 (6) (2012) 746–758, https://

doi.org/10.1016/j.molcel.2012.04.014.
[6] M. Hrdinka, M. Gyrd-Hansen, The met1-linked ubiquitin machinery: emerging themes of (De)regulation, Mol. Cell 68 (2) (2017) 265–280, https://doi.org/10.1016/j.molcel.2017.09.001.
[7] K.P. Foley, B. Desai, A. Vossenkämper, M.A. Reilly, P. Biancheri, L. Wang, D.B. Lipshutz, J. Connor, M. Miller, P.A. Haile, L.N. Casillas, B.J. Votta, P.J. Gough, T.T. MacDonald, C.H. Wouters, C.D. Rose, J. Bertin, OR3–001–RIP2 kinase is activated in Blau syndrome and IBD, Pediatr. Rheumatol. 11 (2013) A3, https://doi.org/10.1186/1546-0096-11-S1-A3.
[8] P.J. Shaw, M.J. Barr, J.R. Lukens, M.A. McGargill, H. Chi, T.W. Mak, T.D. Kanneganti, Signaling via the RIP2 adaptor protein in central nervous system-infiltrating dendritic cells promotes inflammation and autoimmunity, Immunity 34 (1) (2011) 75–84, https://doi.org/10.1016/j.immuni.2010.12.015.
[9] G.M. Argast, N. Fausto, J.S. Campbell, Inhibition of RIP2/RICK/CARDIAK activity by pyridinyl imidazole inhibitors of p38 MAPK, Mol. Cell. Biochem. 268 (2005) 129–140, https://doi.org/10.1007/s11010-005-3701-0.
[10] J.T. Tigno-Aranjuez, J.M. Asara, D.W. Abbott, Inhibition of RIP2's tyrosine kinase activity limits NOD2-driven cytokine responses, Genes Dev. 24 (2010) 2666–2677, https://doi.org/10.1101/gad.1964410.
[11] J.T. Tigno-Aranjuez, P. Benderitter, F. Rombouts, F. Deroose, X. Bai, B. Mattioli, F. Cominelli, T.T. Pizarro, J. Hoflack, D.W. Abbott, In vivo inhibition of RIPK2 kinase alleviates inflammatory disease, J. Biol. Chem. 289 (43) (2014) 29651–29664, https://doi.org/10.1074/jbc.M114.591388.
[12] U. Nachbur, C.A. Stafford, A. Bankovacki, Y. Zhan, L.M. Lindqvist, B.K. Fiil, Y. Khakham, H.J. Ko, J.J. Sandow, H. Falk, J.K. Holien, D. Chau, J. Hildebrand, J.E. Vince, P.P. Sharp, A.I. Webb, K.A. Jackman, S. Muhlen, C.L. Kennedy, K.N. Lowes, J.M. Murphy, M. Gyrd-Hansen, M.W. Parker, E.L. Hartland, A.M. Lew, D.C. Huang, G. Lessene, J. Silke, A RIPK2 inhibitor delays NOD signaling events yet prevents inflammatory cytokine production, Nat. Commun. 6 (2015) 6442, https://doi.org/10.1038/ncomms7442.
[13] P. Canning, Q. Ruan, T. Schwerd, M. Hrdinka, J.L. Maki, D. Saleh, C. Suebsuwong, S. Ray, P.E. Brennan, G.D. Cuny, H.H. Uhlig, M. Gyrd-Hansen, A. Degterev, A.N. Bullock, Inflammatory signaling by NOD-RIPK2 is inhibited by clinically relevant type II kinase inhibitors, Chem. Biol. 22 (9) (2015) 1174–1184, https://doi.org/10.1016/j.chembiol.2015.07.017.
[14] P.A. Haile, B.J. Votta, R.W. Marquis, M.J. Bury, J.F. Mehlmann, R. Singhaus Jr., A.K. Charnley, A.S. Lakdawala, M.A. Convery, D.B. Lipshutz, B.M. Desai, B. Swift, C.A. Capriotti, S.B. Berger, M.K. Mahajan, M.A. Reilly, E.J. Rivera, H.H. Sun, R. Nagilla, A.M. Beal, J.N. Finger, M.N. Cook, B.W. King, M.T. Ouellette, R.D. Totoritis, M. Pierdomenico, A. Negroni, L. Stronati, S. Cucchiara, B. Ziolkowski, A. Vossenkamper, T.T. MacDonald, P.J. Gough, J. Bertin, L.N. Casillas, The identification and pharmacological characterization of 6-(tert-Butylsulfonyl)-N-(5-fluoto-1H-indazil-3-yl)quinoline-4-amine (GSK583), a highly potent and selective inhibitor of RIP2 kinase, J. Med. Chem. 59 (10) (2016) 4867–4880, https://doi.org/10.1021/acs.jmedchem.6b00211.
[15] P.A. Haile, L.N. Casillas, B.J. Votta, G.Z. Wang, A.K. Charnley, X. Dong, M.J. Bury, J.J. Romano, J.F. Mahlmann, B.W. King, K.F. Erhard, C.R. Hanning, D.B. Lipshutz, B.M. Desai, C.A. Capriotti, M.C. Schaeffer, S.B. Berger, M.K. Mahajan, M.A. Reilly, R. Nagilla, E.J. Rivera, H.H. Sun, J.K. Kenna, A.M. Beal, M.T. Ouellette, M. Kelly, G. Stemp, M.A. Convery, A. Vossenkamper, T.T. MacDonald, P.J. Gough, J. Bertin, R.W. Marquis, Discovery of first-in-class receptor interacting protein 2 (RIP2) kinase specific clinical candidate, 2-((4-(Benzo[*d*]thiazol-5-ylamino)-6-(*tert*-butylsulfonyl)quinazolin-7-yl)oxy)ethyl dihydrogen phosphate, for the treatment of inflammatory diseases, J. Med. Chem. 62 (14) (2019) 6482–6494, https://doi.org/10.1021/acs.jmedchem.9b00575.
[16] X. He, S. Da Ros, J. Nelson, X. Zhu, T. Jiang, B. Okram, S. Jiang, P.Y. Michellys, M. Iskandar, S. Espinola, Y. Jia, B. Bursulaya, A. Kreusch, M.Y. Gao, G. Spraggon, J. Baaten, L. Clemmer, S. Meeusen, D. Huang, R. Hill, V. Nguyen-Tran, J. Fathman, B. Liu, T. Tuntland, P. Gordon, T. Hollenbeck, K. Ng, J. Shi, L. Bordone, H. Liu, Identification of potent and selective RIPK2 inhibitors for the treatment of inflammatory diseases, ACS Med. Chem. Lett. 8 (10) (2017) 1048–1053, https://doi.org/10.1021/acsmedchemlett.7b00258.
[17] B. Shairaz, V.M. Carlos, A.O. Rodrigo, D. Ratmir, Preparation of Substituted Benzamides as RIPK2 Inhibitors as Antiinflammatory and Antitumor Agents, 2019. Patent WO 2019161495 A1.
[18] C. Suebsuwong, B. Dai, D.M. Pinkas, A.L. Duddupudi, L. Li, J.C. Bufton, L. Schlicher, M. Gyrd-Hansen, M. Hu, A.N. Bullock, A. Degterev, G.D. Cuny, Receptor-interacting protein kinase 2 (RIPK2) and nucleotide-binding oligomerization domain (NOD) cell signaling inhibitors based on a 3,5-diphenyl-2-aminopyridine scaffold, Eur. J. Med. Chem. 200 (2020) 112417, https://doi.org/10.1016/j.ejmech.2020.112417.
[19] M. Hrdinka, L. Schlicher, B. Dai, D.M. Pinkas, J.C. Bufton, S. Picaud, J.A. Ward, C. Rogers, C. Suebsuwong, S. Nikhar, G.D. Cuny, K.V.M. Huber, P. Filippakopoulos, A.N. Bullock, A. Degterev, M. Gyrd-Hansen, Small molecule inhibitors reveal an indispensable scaffolding role of RIPK2 in NOD2 signaling, EMBO J. 37 (17) (2018) e99372, https://doi.org/10.15252/embj.201899372.
[20] S.W. Cowan-Jacob, G. Fendrich, A. Floersheimer, P. Furet, J. Liebetanz, G. Rummel, P. Rheinberger, M. Centeleghe, D. Fabbro, P.W. Manley, Structural biology contributions to the discovery of drugs to treat chronic myelogenous leukaemia, Acta Crystallogr. D63 (2007) 80–93, https://doi.org/10.1107/S0907444906047287.
[21] R.L. Panek, G.H. Lu, S.R. Klutchko, B.L. Batley, T.K. Dahring, J.M. Hamby, H. Hallak, A.M. Doherty, J.A. Keiser, In vitro pharmacological characterization of PD 166285, a new nanomolar potent and broadly active protein tyrosine kinase inhibitor, J. Pharmacol. Exp. Therapeut. 283 (3) (1997) 1433–1444. jpet.aspetjournals.org/content/283/3/1433.
[22] A.H. Mohedas, X. Xing, K.A. Armstrong, A.N. Bullock, G.D. Cuny, P.B. Yu, Development of an ALK2-biased BMP type I receptor kinase inhibitor, ACS Chem. Biol. 8 (6) (2013) 1291–1302, https://doi.org/10.1021/cb300655w.
[23] A.H. Mohedas, Y. Wang, C.E. Sanvitale, P. Canning, S. Choi, X. Xing, A.N. Bullock, G.D. Cuny, P.B. Yu, Structure-activity relationship of 3,5-diaryl-2-aminopyridine ALK2 inhibitors reveals unaltered binding affinity for Fibrodysplasia Ossificans Progressiva causing mutants, J. Med. Chem. 57 (19) (2014) 7900–7915, https://doi.org/10.1021/jm501177w.
[24] O. Buzko, K.M. Shokat, A kinase sequence database: sequence alignments and family assignment, Bioinformatics 18 (9) (2002) 1274–1275, https://doi.org/10.1093/bioinformatics/18.9.1274.
[25] D.H. Boschelli, Z. Wu, S.R. Klutchko, H.D. Hollis Showalter, J.M. Hamby, G.H. Lu, T.C. Major, T.K. Dahring, B. Batley, R.L. Panek, J. Keiser, B.G. Hartl, A.J. Kraker, W.D. Klohs, B.J. Roberts, S. Patmore, W.L. Elliot, R. Steinkampf, L.A. Bradford, H. Hallak, A.M. Doherty, Synthesis and tyrosine kinase inhibitory activity of a series of 2-Amino-8*H*-pyrido[2,3-*d*]pyrimidines: identification of potent, selective platelet-derived growth factor receptor tyrosine kinase inhibitors, J. Med. Chem. 41 (22) (1998) 4365–4377, https://doi.org/10.1021/jm980398y.
[26] S.R. Klutchko, J.M. Hamby, D.H. Boschelli, Z. Wu, A.J. Kraker, A.M. Amar, B.G. Hartl, C. Shen, W.D. Klohs, R.W. Steinkampf, D.L. Driscoll, J.M. Nelson, W.L. Elliot, B.J. Roberts, C.L. Stoner, P.W. Vincent, D.J. Dykes, R.L. Panek, G.H. Lu, T.C. Major, T.K. Dahring, H. Hallak, L.A. Bradford, H.D. Hollis Showalter, A.M. Doherty, 2-Substituted Aminopyrido[2,3-*d*]pyrimidin-7(8*H*)-ones. Structure-activity relationships against selected tyrosine kinases and in vitro and in vivo anticancer activity, J. Med. Chem. 41 (17) (1998) 3276–3292, https://doi.org/10.1021/jm9802259.
[27] G.A. Kraus, V. Gupta, M. Mokhtarian, S. Mehanovic, M. Nilsen-Hamilton, New effective inhibitors of the Abelson kinase, Bioorg. Med. Chem. 18 (17) (2010) 6316–6321, https://doi.org/10.1016/j.bmc.2010.07.021.
[28] Jaekyoo, L.; Jang-Sik, J.; Hae-Jun, H.; Ho-Juhn, S.; Jung-Ho, K.; Se-Won, K.; Jong Sung, K.; Jaesang, L.; Tae-Im, L.; Yung-Geun, C.; Sung-Ho, P.; In Yong, L.; Byung-Chul, S.; Paresh Devidas, S.; Dong-Sik, J. Substituted pyrimidine compounds and their use as SYK inhibitors. Patent WO2015061369 A1, 2015.
[29] S.N. VanderWel, P.J. Harvey, D.J. McNamara, J.T. Repine, P.R. Keller, J. Quin 3rd, R.J. Booth, W.L. Elliott, E.M. Dobrusin, D.W. Fry, P.L. Toogood, Pyrido[2,3-d] pyrimidin-7-ones as specific inhibitors of cyclin-dependent kinase 4, J. Med. Chem. 48 (7) (2005) 2371–2387, https://doi.org/10.1021/jm049355.
[30] A.K. Charnley, M.A. Convery, A. Lakdawala Shah, E. Jones, P. Hardwicke, A. Bridges, M. Ouellette, R. Totoritis, B. Schwartz, B.W. King, D.D. Wisnoski, J. Kang, P.M. Eidam, B.J. Votta, P.J. Gough, R.W. Marquis, J. Bertin, L. Casillas, Crystal structures of human RIP2 kinase catalytic domain complexed with ATP-competitive inhibitors: foundations for understanding inhibitor selectivity, Bioorg. Med. Chem. 23 (21) (2015) 7000–7006, https://doi.org/10.1016/j.bmc.2015.09.038.
[31] C.E. Sanvitale, G. Kerr, A. Chaikuad, M.-C. Ramel, A.H. Mohedas, S. Reichert, Y. Wang, J.T. Triffitt, G.D. Cuny, P.B. Yu, C.S. Hill, A.N. Bullock, A new class of small molecule inhibitor of BMP signaling, PloS One 8 (4) (2013), e62721, https://doi.org/10.1371/journal.pone.0062721.
[32] A. Degterev, Z. Huang, M. Boyce, Y. Li, P. Jagtap, N. Mizushima, G.D. Cuny, T.J. Mitchison, M.A. Moskowitz, J. Yuan, Chemical inhibitor of nonapoptotic cell death with therapeutic potential for ischemic brain injury, Nat. Chem. Biol. 1 (2) (2005) 112–119, https://doi.org/10.1038/nchembio711.
[33] G.D. Cuny, A. Degterev, RIPK protein kinase family: atypical lives of typical kinases, Semin. Cell Dev. Biol. (2020) S1084–S9521, https://doi.org/10.1016/j.semcdb.2020.06.014.
[34] T. Anastassiadis, S.W. Deacon, K. Devarajan, H. Ma, J.R. Peterson, Comprehensive assay of kinase catalytic activity reveals features of kinase inhibitor selectivity, Nat. Biotechnol. 29 (11) (2011) 1039–1045, https://doi.org/10.1038/nbt.2017.
[35] M. Hrdinka, B.K. Fiil, M. Zucca, D. Leske, K. Bagola, M. Yabal, P.R. Elliott, R.B. Damgaard, D. Komander, P.J. Jost, M. Gyrd-Hansen, CYLD limits Lys63- and Met1-linked ubiquitin at receptor complexes to regulate innate immune signaling, Cell Rep. 14 (12) (2016) 2846–2858, https://doi.org/10.1016/j.celrep.2016.02.062.